The emergence of hydrogeophysics for improved understanding of subsurface processes over multiple scales

Andrew Binley[1]*, Susan S. Hubbard[2], Johan A. Huisman[3], André Revil[4,5], David A. Robinson[6], Kamini Singha[7], Lee D. Slater[8]

[1]Lancaster Environment Centre, Lancaster University, Lancaster LA1 4YQ, UK
[2] Lawrence Berkeley National Laboratory, Berkeley, CA USA
[3] Agrosphere institute (IBG 3), Forschungszentrum Jülich GmbH, Jülich, Germany
[4] Department of Geophysics, Colorado School of Mines, Golden, CO, USA
[5] ISTerre, CNRS, UMR CNRS 5275, Université de Savoie, Le Bourget du Lac, France
[6] Soils, Land & Ecohydrology, Centre for Ecology & Hydrology, Bangor, UK
[7] Department of Geology and Geological Engineering, Colorado School of Mines, Golden, CO, USA
[8] Department of Earth & Environmental Sciences, Rutgers-Newark, NJ, USA

*corresponding author: a.binley@lancaster.ac.uk

Abstract

Geophysics provides a multi-dimensional suite of investigative methods that are transforming our ability to see into the very fabric of the subsurface environment, and monitor the dynamics of its fluids and the biogeochemical reactions that occur within it. Here, we document how geophysical methods have emerged as valuable tools for investigating shallow subsurface processes over the past two decades and offer a vision for future developments relevant to hydrology and also ecosystem science. The field of "hydrogeophysics" arose in the late 1990s, prompted, in part, by the wealth of studies on stochastic subsurface hydrology that argued for better field-based investigative techniques. These new hydrogeophysical approaches benefited from the emergence of practical and robust data inversion techniques, in many cases with a view to quantify shallow subsurface heterogeneity and the associated dynamics of subsurface fluids. Furthermore, the need for quantitative characterization stimulated a wealth of new investigations into petrophysical relationships that link hydrologically relevant properties to measurable geophysical parameters. Development of time-lapse approaches provided a new suite of

tools for hydrological investigation, enhanced further with the realization that some geophysical properties may be sensitive to biogeochemical transformations in the subsurface environment, thus opening up the new field of "biogeophysics". Early hydrogeophysical studies often concentrated on relatively small 'plot-scale' experiments. More recently, however, the translation to larger-scale characterization has been the focus of a number of studies. Geophysical technologies continue to develop, driven, in part, by the increasing need to understand and quantify key processes controlling sustainable water resources and ecosystem services.

Introduction

The ability to observe the fabric of the subsurface environment and processes that occur within it remains a challenge in many branches of science and engineering. This is particularly the case for hydrology, where the transport and transformation of fluids in the shallow subsurface (commonly < 100 m deep) are governed by interactions between physical, biological and geochemical processes occurring in highly heterogeneous and often variably saturated soils, sediments and bedrock compartments (Figure 1). These complex and multi-scale interactions are difficult to observe and thus hinder our ability to understand, predict and ultimately manage shallow systems in a sustainable manner. The need to improve our understanding of processes within the subsurface environment exists due to several drivers, including: demands on provision of suitable quantities of groundwater at appropriate quality; determining the legacy of industrial, agricultural and military sources of groundwater contamination; quantifying terrestrial carbon cycling feedbacks to climate; ensuring food security; and understanding water resource impacts on ecosystem function. Hydrogeophysics provides a suite of tools that may assist in addressing such drivers through the quantification of the structure and function of the shallow subsurface (Figure 1).

INSERT FIGURE 1 NEAR HERE

Traditional in-situ 'point scale' sampling of the subsurface for system properties (e.g. permeability) and states (e.g. water content, ion concentrations, redox potential) has been widely based on invasive drilling approaches, through the recovery of samples (e.g., cores) and installation of fluid sampling apparatus. Whilst such approaches may be relatively easy in the very near surface (< 1m), their financial (and labor) costs often constrain such investigations at greater depths, enforcing an interpretation

based on few observations and at shallow depths. These measurements are also limited by the scale of measurement they offer, as it is widely accepted that the subsurface process or property under investigation (e.g. permeability) can be scale dependent [e.g., Schulze-Makuch et al., 1999], particularly in fractured media. Furthermore, in some instances, invasive sampling of the subsurface is severely restricted, for example due to inaccessibility caused by features on the ground surface (e.g. built infrastructure), environmental protection constraints, the hazardous nature of a site, or the threat of disturbing and transforming contaminant pathways through an invasive activity. For these reasons, geophysical methods, many of which were originally developed for oil and mineral exploration, have emerged as valuable tools for supporting investigation of the shallow subsurface and for monitoring the dynamics of hydrological and biogeochemical processes that occur within it.

Several geophysical methods have been used in hydrological investigations for decades. Geophysical well logging, for example, is well established and routinely used to assist drilling operations through the recording of lithological geophysical descriptors, thus helping the development of hydrogeological conceptualizations at a site. However, over the past two or three decades new geophysical methods have emerged (or have developed significantly), several of which have proved to be extremely effective in providing valuable information about the subsurface environment beyond the borehole wall. New approaches have been developed to exploit the information attainable from these techniques, supported by new insights into relationships between properties of interest and observable geophysical properties. During the 1990s, “hydrogeophysics” arose as an interdisciplinary field that focuses on the improved understanding of hydrological processes through geophysical observations. Whilst initially focused on aiding in the development of conceptual subsurface models, applications of hydrogeophysics have developed to provide new insight into subsurface mechanisms, to aid in the parameterization of subsurface flow and transport models, and to advance new tools for monitoring the hydrological and biogeochemical status of the subsurface environment.

Several key challenges exist in translating geophysical measurements into information that is useful for improving our understanding and management of shallow subsurface systems. First and foremost, geophysical measurements do not generally provide direct information about hydrogeological properties or states and as such, their effective use is governed by the strength of the relationships between estimated geophysical properties and the properties of interest. In addition, they can suffer from limitations of measurement scale and resolution in that the target to be characterized may be

much smaller than the footprint of the geophysical measurement. Profound understanding of these factors is essential for successful application, and motivates the existence and continued evolution of hydrogeophysics as a research field.

Many of the key advances in hydrogeophysics have been documented in *Water Resources Research*; Figure 2 illustrates the growth of hydrogeophysics activity in the journal since 1990. The number of hydrogeophysics-related papers has continued to grow at an almost constant rate (Figure 2a) and now accounts for typically 5 - 6% of the journal content (Figure 2b). We use this celebratory issue to reflect on the emergence of the field through publications in the journal and the wider literature.

INSERT FIGURE 2 NEAR HERE

In this review, we first introduce the commonly used geophysical methods for hydrological investigations and outline the principles of geophysical data inversion and measurement scale. We then discuss developments in hydrogeophysical relationships, which underpin successful application of hydrogeophysics. Early approaches of geophysical methods to hydrology based on characterizing structure are reviewed, followed by subsequent developments addressing temporal dynamics, biogeochemical processes and applications to ecosystem science. We then offer a vision for the future direction of hydrogeophysics.

Geophysical methods

A range of geophysical methods have been used effectively in hydrological investigations. Details of such methods can be found in many texts [e.g. Rubin and Hubbard, 2005; Vereecken et al., 2006; Robinson et al.,2008a]; we restrict this review to the general concepts. Within most methods a geophysical property (or properties) of the subsurface is evaluated using sensors deployed on the boundary of the area of study in response to a natural or activated source. A link between such a property and a hydrological property or state is clearly essential to using these data for hydrologic inference, as discussed later. Assuming such a link exists, the success of the method then relies on the ability to infer variations in the property (or state) of interest from the accuracy- and resolution-limited geophysical parameter(s). The most commonly used methods for hydrological applications (in no particular order) are: direct current (DC) resistivity, induced polarization (IP), self-potential (SP), ground penetrating radar (GPR),

128 electromagnetic induction (EMI), seismic refraction, nuclear magnetic resonance (NMR) and
129 microgravity. (Note that we use the term induced polarization here to capture a broad range of
130 polarization measurement methods; IP is often used to define a time-domain measurement and
131 complex resistivity is commonly used as a reference to measurements in the frequency domain, whilst
132 spectral induced polarization (SIP) refers to the measurement of the frequency spectrum of complex
133 resistivity). Table 1 lists the geophysical properties that these methods provide and the hydrological
134 properties that have commonly been derived from these geophysical properties. Note that we have not
135 included temperature sensing as a geophysical approach here, although we recognize the immense
136 success in developments of such approaches for hydrological investigations [e.g. Hatch et al., 2006;
137 Selker et al., 2006; Keery et al., 2007; Tyler et al., 2009].
138
139 INSERT TABLE 1 NEAR HERE
140
141 Several methods can be deployed in various configurations, allowing the user to tailor the survey to
142 optimize the sensitivity. Electrical methods (DC resistivity, IP, SIP, SP), which involve making
143 measurements using electrodes with galvanic or capacitive contact with the subsurface, allow significant
144 flexibility in terms of acquisition configuration for plot-scale (<10 m deep) investigations. Most early
145 applications of electrical methods in hydrology were based on surface-based configurations originally
146 developed for resource exploration. However, the inherent adaptability of the basic configuration to
147 target the problem of interest led to deployment in alternative configurations, e.g. in boreholes [e.g.
148 Daily et al., 1992; Singha and Gorelick, 2005], or surrounding a column or object under examination, as
149 in laboratory or lysimeter based studies [e.g. Binley et al., 1996; Koestel et al., 2008]. In some cases,
150 deployment in contact with the water surface above the area of investigation (i.e. water-borne) has
151 proved to be effective [e.g., Slater et al., 2010].
152
153 Geophysical methods based on electromagnetic induction (EMI) offer greater range of both application
154 and scale of investigation than electrical methods. These methods may be deployed on the ground
155 surface (manually or using towed platforms), in boreholes, and also in an airborne manner. Depth of
156 investigation is controlled by varying the excitation frequency or separation of electromagnetic coils.
157 Alternatively, depth information may also be obtained from the analysis of time-dependency in a
158 measured transient signal response [Keller and Frischknecht, 1966].
159

GPR methods are based on the recording of high frequency electromagnetic signals transmitted into the ground. Ground-based surveys are used to sense signals that are either directly transmitted between antennas at shallow depths or reflected from greater depths to return to the ground surface; cross-borehole surveys, in contrast, measure transmitted energy between boreholes [Huisman et al., 2003]. Reflection mode GPR can also be applied in single boreholes, as demonstrated, for example, by Dorn et al. [2011]. The popularity of GPR in hydrogeophysics can be attributed to the relatively high spatial resolution and the direct connectivity between radar velocity and moisture content [Topp et al., 1980]. However, in most environments the depth of investigation of ground based GPR is limited to a few meters because of the high attenuation of electromagnetic energy in electrically conductive porous media. GPR methods can also be used to determine information about the electrical conductivity of the subsurface, given the measurement of signal attenuation at the receiver.

Seismic methods measure the velocity and attenuation of seismic waves in order to infer information about mechanical properties of the subsurface. Like GPR, seismic methods are based on the transmission of an energy source (originating, for example, from a sledgehammer at the surface) and the measurement of a signal at a receiver (geophone). Again, like GPR, seismic methods may be used in a ground-based or cross-borehole configuration. New techniques have been developed to exploit the link between seismic and electromagnetic energy [Revil et al., 2014a; Sava et al., 2014].

The SP method is a passive method (i.e. there is no applied source of signal) that probes directly non-equilibrium thermodynamic processes in the subsurface. A major application of SP measurements in hydrology is sensing the flow of the ground water, which drags the excess of ionic charges located in the vicinity of a charged mineral surface and therefore produces a (streaming) electrical current [Abaza and Clyde, 1969; Revil et al., 2003]. This approach has proven useful for estimating hydraulic properties during pumping tests [e.g. Darnet et al., 2003] and hydraulic tomography [Ahmed et al., 2014] or for mapping preferential flowpaths [Ikard et al., 2012].

A relatively new geophysical technique that has shown potential for hydrological applications is nuclear magnetic resonance (NMR). Measurements can be made using downhole sondes, although the surface-based sounding (called magnetic resonance sounding (MRS), or surface NMR (SNMR)) can provide 1D and 2D models of hydraulic properties to depths of several tens of meters [e.g. Herckenrath et al., 2012; Vilhelmsen et al., 2014].

In contrast to NMR, gravimetry is a well-established geophysical technique. The method was originally developed for exploration and geodesy purposes. Gravimeters can sense differences in gravity caused by local variations in density. The temporal variability in gravimetry measurements offers the greatest value of this technique in hydrogeophysical studies. Such variation due to groundwater level changes has been studied in detail since, for non-hydrological applications, this contributes a significant noise component. Such 'noise' can thus represent 'signal' for monitoring groundwater storage changes [e.g., Gehman et al., 2009] and constraining hydraulic parameter estimates [e.g., Blainey et al., 2007]. We also note the immense impact of the Gravity Recovery and Climate Experiment (GRACE) satellite-based gravimetry measurements on large scale observations of water storage and groundwater depletion in aquifers [e.g., Yeh et al., 2006; Fen et al., 2013], although we limit this review to land-based and airborne approaches.

A wide range of geophysical methods therefore exists, allowing us to investigate the subsurface at a range of spatial scales in a variety of survey configurations. As discussed later, some of these methods offer direct insight into the hydrological characteristics of the subsurface; furthermore, a number of methods are well-suited to studying the temporal variability of subsurface processes.

Data inversion

Typically, geophysical surveys are conducted to assess the spatial variability of a property (or changes in a property) within the study region. The translation of raw geophysical measurements to spatial patterns of geophysical parameters is usually achieved through an inversion process (Figure 3). In the 1980s, rapid growth in available computer resources needed for such inversion prompted numerous developments in inversion algorithms, leading to widely available tools that are now robust, and in many cases, capable of rapid production of 2D and 3D images of the subsurface.

INSERT FIGURE 3 NEAR HERE

Often the inversion of geophysical data is challenging because of ill-posedness and non-uniqueness, and typically some stabilizing mechanism is needed. Originating from exploration and deep Earth studies, the introduction of regularization functions to address problems of ill-posed, non-unique solutions by minimizing the roughness of an image [e.g. Tikhonov and Arsenin, 1977; Constable et al., 1987;

Tarantola, 2005] transformed the robustness of geophysical inverse codes and opened up some of the geophysical methods (in particular electrical methods) to a broader user base. Such approaches often naturally lead to smoothed images of some geophysical property, which can be argued as introducing *a priori* information about the subsurface as we may expect there to be some autocorrelation of properties over length scales. However, such approaches do not typically account for our quantitative knowledge of spatial variability of properties: they recognize that it exists but in many approaches the level of smoothing does not necessarily honor explicitly the geostatistical information that may be known about the subsurface. More sophisticated inverse methods that do consider such prior information on subsurface heterogeneity have been developed in hydrogeophysics [Hyndman et al., 1994; Eppstein and Dougherty, 1998; Yeh et al., 2002; Linde et al., 2006; Hermans et al., 2012]. Introducing such additional knowledge (or assumed knowledge) of the subsurface in the inversion can have a dramatic effect on the resultant images: the spatial structure can be significantly enhanced. However, such approaches have to date been limited to synthetic studies or extremely well characterized research sites as applied to hydrologic systems.

Large-scale (e.g. airborne) investigations introduce further challenges for the inversion process due to the size of datasets. Traditionally, in airborne EMI surveys, maps of apparent electrical conductivity data would be constructed or individual soundings analyzed as 1D (conductivity-depth) models. However, developments in laterally constrained inversion methods [e.g. Auken and Christiansen, 2004] permit large scale quantitative modelling of the subsurface using airborne acquired data [e.g. Siemon et al., 2009]. The computational constraints of solving large-scale inverse problems for a wide range of geophysical problems has prompted developments in the use of wavelet transformations to reduce the density of the sensitivity matrix [e.g., Li and Oldenburg, 2003], seek adaptive mesh parameterization [e.g., Davis and Li, 2011] and exploit highly parallel computation [e.g. Cuma and Zhdanov, 2014]. There has also been a migration towards unstructured meshes that permit better adaptation to geological structures and topography, prompting the development of new regularization strategies [e.g., Lelièvre and Farquharson, 2013] that can exploit such flexible discretization of the subsurface.

Most inversion applications in hydrogeophysics have focused on the analysis of a single geophysical modality (e.g. DC resistivity); however, joint inversion of data from multiple geophysical data types may generate greater information about the subsurface. In its simplest form, joint inversion may focus on a simultaneous inversion of geophysical data sensitive to a common property (e.g. electrical conductivity).

Monteiro Santos et al. [2007] illustrated such an approach for 2D imaging of resistivity using DC resistivity and audio-magnetotelluric data. In a petrophysical approach, geophysical parameters are linked through rock properties (such as porosity or water content) to constrain the inversion. In this approach, the problem is often solved with *a priori* knowledge of some physical relationships between the parameters controlling the geophysical data [e.g. Hoversten et al., 2006]. The drawback of this approach is that the final model is a function of the *a priori* relationship, which may be poorly known and not necessarily constant within the area of investigation. In a structural approach it is assumed that spatial changes in geophysical parameters are related, irrespective of any common petrophysical relationship, i.e. changes in one parameter should coincide with changes in another parameter. The simple concept of cross-gradient constraints introduced by Gallardo and Meju [2003] has provided a flexible approach for addressing structural inversion of geophysical data [see also review by Gallardo and Meju, 2011]. Linde et al. [2006] illustrated the use of this approach in hydrogeophysics, using cross-borehole DC resistivity and GPR data. The resulting jointly inverted images (Figure 4) were then analyzed to determine bivariate trends in electrical conductivity and permittivity, revealing different lithological units at the study site.

INSERT FIGURE 4 NEAR HERE

As discussed later, studying the temporal dynamics of geophysical signals can provide improved knowledge of the system's behavior. Data inversion techniques have developed to exploit such approaches. Early methods relied on relatively simple comparisons of two datasets [e.g. Daily and Owen, 1991; LaBrecque and Yang, 2001]. More recently, approaches have been developed to invert multiple time-lapse datasets simultaneously [e.g., Kim et al. 2009; Karaoulis et al. 2011].

One may consider a geophysical image as a proxy for the spatial distribution of a property of interest (e.g. permeability) and traditionally geophysical data were used in this way, i.e. the flow of information is one way: from geophysics to hydrology. However, provided adequate knowledge of the relationship between geophysical and hydrological properties (or states) is known (through petrophysical transforms) then the inversion can be cast in a coupled manner, whereby a hydrological model generates proposals (e.g. the distribution of soil water content) and the consistency with observed geophysical measurements is evaluated (often in combination with other data). Thus the hydrological model constrains the inversion and the final result is guaranteed to be consistent with the hydrological

conceptualization. Such an approach may be considered to be a truly coupled hydrogeophysical inversion as feedback between geophysics and hydrology is explicitly defined. Furthermore, artifacts resulting from traditional (potentially unphysical) regularized geophysical inversion are eliminated. Kowalsky et al. [2005] documented one of the first attempts at following such a coupled approach, using cross-well GPR data to estimate soil water content in the vadose zone. Other examples following similar concepts include those of: Looms et al. [2008]; Hinnell et al. [2010]; Huisman et al. [2010]; Irving and Singha [2010]; Scholer et al. [2011]; Pollock and Cirpka [2012]; Jardani et al. [2013]; Vilhelmsen et al. [2014]. A further advantage of these methods is the natural ability to incorporate other data sources within the inversion; thus the geophysical data merely represent one of several possible data sources. The disadvantages of such coupled inversion approaches are (1) greater computational burden, and (2) the reliance on uncertain petrophysical relationships linking geophysical and hydrological quantities. Moreover, adopting such an approach enforces the prior hydrological conceptualization and thus relies on adequate confidence in the hydrological conceptual model. In some cases one may wish to explore the geophysical data independent of prior hydrological conceptualizations to reveal new insight rather than simply affirm prior assumptions of a system.

Oware et al. [2013] offer an interesting alternative to the coupled approach by training images generated from a hydrogeological model within a framework that solves for sets of geophysical parameters with overall reduced dimensionality. They demonstrate that, under conditions of high uncertainty in the underlying hydrogeological model, their approach is superior to conventional smoothed or coupled inversions. Others have solved directly for hydrologic parameters of interest, such as plume moments or geometry [Day-Lewis et al., 2007; Miled and Miller, 2007; Pidlisecky et al., 2011], effective velocity and dispersivity [Koestel et al., 2008]. As in many areas of natural science, data may be used to support or to illuminate: the choice of inversion scheme will depend on the focus of the investigation and the level of *a priori* knowledge of the system.

Measurement scale

As noted earlier, a significant advantage of geophysical measurements over many traditional subsurface observational approaches is the greater measurement support volume that they offer. Western et al. [2002] already highlighted that the limited support volume of conventional sensors can constrain the value of hydrological process data.

We consider two aspects of measurement scale here. First, by conducting geophysical surveys over transects along the surface, or, for example, between boreholes, we can assess variability over some survey scale. Second, each individual geophysical measurement is an integrated measure, with its own support scale. The latter will constrain the spatial resolution achievable from the method, but has the advantage of characterizing properties over scales that may be more representative of the hydrological property or process under investigation. For example, the measurement of the time of flight of a radar signal between two boreholes is sensitive to the total water content along the pathway from transmitter to receiver. Thus, such a measurement can provide an integrated water content measure over several meters [e.g. Parkin et al., 2000; Binley et al., 2001; Strobach et al., 2014]. Similarly, developments in surface-based GPR based on measurement of direct waves travelling close to the ground surface [e.g. Huisman et al., 2001; Grote et al., 2003] or using above ground sensors [e.g. Lambot et al., 2006], offer the capability of providing mobile soil moisture sensors that sample larger volumes than normally achievable with standard point sensors. This enhanced measurement support volume is often overlooked, although it does present challenges as we strive to assess these new techniques but are constrained by verification from 'acceptable' measurement approaches based on a much smaller spatial scale [e.g. Huisman et al., 2002].

The survey scale for geophysical techniques varies considerably. Some methods (e.g. surface deployed GPR, frequency domain EMI) are fully mobile and can often provide information without the need for data inversion over extensive areas. Frequency domain EM tools are particularly well suited to vehicle-towed platforms [e.g. Sudduth et al., 2001; André et al., 2012]. Others, for example, electrical and seismic methods, use grounded multi-sensors on cable arrays that limit the mobility of measurement arrays, as does the survey time required for an individual measurement. Time domain EMI and NMR can require extensive setup periods for ground-based surveys, again limiting mobility. Attempts have been made to develop mobile land-based platforms, particularly for electrical methods. Panissod et al. [1997] and Christensen and Sørensen [2001], for example, illustrated different approaches using vehicle towed electrical arrays, which have proved effective, particularly for relatively shallow investigations. Allred et al. [2008] discuss other vehicle-mounted electrical measurement systems. Water-borne surveys can also be effective for greater scale of investigation. Rucker et al. [2011], for example, completed over 660 line kilometers along the Panama Canal, using a 170m long floating electrode array.

As noted earlier, EMI methods can be used on airborne platforms. As in many other geophysical methods, airborne electromagnetic methods were originally developed for mineral resource exploration, however, the value of these techniques for large-scale hydrogeological studies is now well established. Cook and Kilty [1992] illustrated the use of helicopter-borne frequency domain EMI (FDEM) surveys for mapping recharge rates over an area of 32 km^2 in south east Australia. They established an inverse relationship between subsurface electrical conductivity and recharge rate (due to leached salts and low water content in highly recharged areas) and thus were able to utilize maps of the variation in electrical conductivity in the top few tens of meters of the subsurface to obtain immensely valuable hydrogeological information. Paine [2003] illustrated the effectiveness of FDEM surveys for mapping groundwater salinization over a 35 km^2 area. Kirkegaard et al. [2011] utilized helicopter-borne time domain electromagnetic (TDEM) surveys to identify zones of low salinity groundwater discharging into a coastal lagoon in Denmark. Such examples demonstrate the immense power of airborne methods for surveying at regional scales.

Geophysical methods are often compared based on a measure of achievable horizontal survey scale; however, one also needs to consider the vertical (depth) scale of sensitivity that can be practically achieved. To illustrate this, Figure 5 shows a typical horizontal and vertical scale achievable in one day for three different methods (ERT, FDEM, TDEM) of sensing the spatial variation in electrical conductivity. For this comparison we assume: (i) a two person field crew; (ii) land-based application, not vehicle mounted; (iii) easily accessible terrain; (iv) a single transect survey. The comparison of horizontal and vertical scales shown in Figure 5 demonstrates the range achievable from different geophysical methods, which is important to consider in selecting an appropriate method for a given problem. FDEM methods may offer significant horizontal coverage but can lack depth of investigation, in contrast ground-based TDEM provides superior depth of investigation but mobility is more restricted than FDEM and thus horizontal coverage is limited. ERT offers greater flexibility in horizontal and vertical coverage by adjusting electrode spacing. The examples in Figure 5 show spatial coverage for 1 m and 5 m electrode spaced ERT arrays: greater depth of investigation is achievable for larger spacing of electrodes, although both horizontal and vertical resolution deteriorates.

INSERT FIGURE 5 NEAR HERE

Hydrogeophysical relationships

Constitutive relationships that link measured geophysical parameters to hydrological properties (or states) are essential for reliable hydrological interpretation of geophysical data (Figure 6). A number of relationships have long been established [e.g. Archie, 1942]; however, over the past two decades we have seen significant exploration into new theoretical or empirical models connecting hydrogeological properties and processes to geophysical observables. Some of this work has been driven by new insight into microscale mechanisms, new ways of simulating the effective properties of porous media, and also the arrival of new measurement techniques.

INSERT FIGURE 6 NEAR HERE

The work of Topp et al. [1980] (the second most cited paper in *Water Resources Research*) provided empirical polynomial relationships for mineral and organic soil that link soil moisture to dielectric properties or permittivity. The models underpin the now routinely used time domain reflectometry (TDR) method for soil water content measurement [Robinson et al., 2003] but also provide a valuable relationship for linking GPR-derived radar velocities to soil moisture content, since the radar velocity is inversely proportional to permittivity. Further studies of soil permittivity [Saarenketo, 1998] and rock permittivity [Chelidze and Gueguen, 1999] have explored frequency dependence (for example in the experimental studies of West et al. [2003], the effective medium modeling work of Chen and Or [2006], or the volume averaging approach of Revil [2013]), which is important to develop appropriate relationships for typical GPR frequencies (often lower than those used for TDR). Investigations of, and insight into, links between soil water content and electrical conductivity of porous media have also continued [e.g. Mualem and Friedman, 1991; Roberts and Lin, 1997; Brovelli et al., 2005; Revil, 2013]. An improved understanding of the role of textural properties on bulk permittivity and conductivity behavior has also been achieved [Friedman and Robinson, 2002; Brovelli and Cassiani, 2011]. Whilst most investigations exploring rock physics relations for GPR have focused on classical porous media, Comas and Slater [2007] and Parsekian et al. [2012] examined the unique characteristics of peat in order to derive ways of estimating biogenic gas content in peat bogs using permittivity measurements derived from GPR.

Most constitutive relationships for GPR have been developed at the scale of a representative homogenous medium; however, several researchers have identified potential bias in assuming these relations hold in layered [e.g. Chan and Knight, 1999; Robinson et al., 2005] or heterogeneous [e.g. Moysey and Knight, 2004] media, with clear implications for interpretation of field data.

Models that link permeability to measurable geophysical properties have been the quest of many researchers over the past few decades, and continue to drive many hydrogeophysics studies. As illustrated by Worthington [1977], Urish [1981] and Purvance and Andricevic [2000], electrical conductivity and permeability relationships do not universally hold because of the surface conduction mechanisms in finer grained media. Recognizing this, Revil and Cathles [1999] provided a mechanistic framework for linking electrical conductivity and permeability in both clean and shaly sands; Doussan and Ruy [2009] later proposed the incorporation of a measurement of clay content to account for such surface conduction (although we note here that the clay mineralogy, not only the content, is important in accounting for surface conduction). Even totally clean (clay-free) rock formations exhibit an appreciable amount of surface conductivity for fresh water aquifers [see Revil et al., 2014b], a point often neglected in hydrogeophysics. The challenges associated with electrical conductivity-permeability models have driven recent research into utilizing measures of the ability of the porous medium to polarize electrically to infer permeability.

Induced polarization (IP) is a well-established technique, originally developed for mineral exploration, which provides a measure of how well a material polarizes due to an applied electrical field. If we assume that the polarization occurs along the (charged) grain boundary, or at pore throat constrictions, then the extent of polarization is related to geometrical characteristics of the pore space that also influence permeability. Thus while electrical conductivity is principally sensitive to the pore volume and its connectivity, IP offers an additional measure of a grain/pore throat size effect. Slater and Lesmes [2002] illustrated the link, in an empirical sense, between a measure of polarization and permeability in unconsolidated sediments. Slater et al. [2014] extended this further for highly permeable sands and gravel mixtures in a cobble framework. This recent study highlights some of the limitations of using IP: whilst it may be possible to differentiate low permeability and high permeability units, to accurately resolve permeability in a coarse grained matrix is extremely challenging in a field setting given the weak polarization characteristic of such media relative to the resolving power of current field instrumentation.

445 Extending IP measurements into the frequency domain permits an assessment of the time (or
446 distribution of times) taken for the electrical polarization to return to equilibrium (i.e. relaxation times).
447 Binley et al. [2005] explored such measurements in their study of sandstone permeability and
448 illustrated, for the first time, a clear positive relationship between a measure of an effective electrical
449 relaxation time and permeability. Revil et al. [2012a] developed an approach connecting the relaxation
450 times of IP and the intrinsic formation factor to permeability. The relationships developed were,
451 however, empirical and their universality is questionable. Developments of mechanistic models,
452 however, have started to provide some insight into the potential link between IP measurements and
453 permeability [e.g. Revil, 2012; 2013] (Figure 7).
454
455 INSERT FIGURE 7 NEAR HERE
456
457 More mechanistic models are also being developed in order to fully exploit the possible value of using
458 measurements of patterns of the natural voltage (SP) in the subsurface to infer hydrological states, for
459 example, water table elevations [Revil et al., 2003] and pore water velocity [Ikard et al., 2012]. Revil and
460 Mahardika [2013] took such approaches further by also considering seismoelectric sources in their
461 unified, coupled model of hydromechanical and electromagnetic disturbances in porous media. They
462 provided a general framework that might be used with harmonic pumping tests to jointly invert
463 hydraulic heads, ground deformation, and SP signals in order to image permeability and the specific
464 storage around wells in confined and unconfined aquifers.
465
466 Geophysical use of NMR was originally developed in the oil industry. These measurements directly sense
467 the water component, as, when hydrogen atoms located in a static magnetic field are stimulated by a
468 secondary alternating electromagnetic field, they produce a magnetic field.Studies into the links
469 between NMR signals and pore size distributions [e.g. Hinedi et al., 1993,1997; Stingaciu et al., 2010;
470 Mohke and Hughes, 2014] and extensions to water retention models [Costabel and Yaramanci, 2013]
471 have been explored. It is perhaps the potential of using these measurements to infer permeability [e.g.
472 Ionnidis et al., 2006; Gladkikh et al., 2007; Dlubac et al., 2013] that offers the greatest possible impact.
473 As in the case of electrically-based models, NMR-permeability relationships still remain empirically
474 based and are likely to be site-specific.
475

476 Recognizing the potential sensitivity of geophysical properties to subsurface contamination, a number of
477 studies have explored the geophysical response to changes in groundwater quality, particularly for non-
478 aqueous phase liquids. Hedberg et al. [1993] demonstrated the sensitivity of NMR measurements to the
479 different fluid phases of gasoline-saturated sandstone, while Li et al. [2001] illustrated how the bulk
480 dielectric behavior of soils is affected by the sorption of oil onto the grain surface. In their experimental
481 study, Shefer et al. [2013] revealed the effect of decane (as a non-aqueous phase) on the electrical
482 polarization of soils, showing an apparent change in the dominant relaxation time of the sample as the
483 concentration of decane changed. The SP method has also been used with success to determine the
484 redox potential of some organic-rich contaminant plumes [Revil et al., 2010]. Minsley et al. [2007]
485 showed, through a field-based investigation, how SP measurements are sensitive to tetrachloroethylene
486 (PCE) and trichloroethylene (TCE) contamination at the Savannah River field site, although they
487 acknowledge that more insight into the mechanisms influencing measurable natural voltages in the
488 subsurface is needed. In fact, most studies to date on contaminant-geophysical behavior have been
489 purely empirical and an overarching physicochemical model that explains observed geophysical signals is
490 currently lacking. Given the complexity of physicochemical processes within contaminated porous
491 media, the search for universal models that link geophysical signals to contaminant characteristics is
492 likely to be futile.
493

494 ## Characterizing hydrogeological heterogeneity with static geophysical data

495

496 During the late 1970s/ early 1980s the role of aquifer heterogeneity on solute transport in groundwater
497 was realized, along with the inadequacy of traditional lumped representations of aquifer properties for
498 predicting the fate of subsurface contaminants [e.g. Gelhar, 1986]. A large number of studies explored
499 these issues in the new field of 'stochastic groundwater hydrology', mainly focusing on the impact of
500 spatial variability in hydraulic conductivity on solute transport and the possible representation of such
501 heterogeneity through effective parameters [e.g. Pickens and Grisak, 1981; Gelhar and Axness, 1983;
502 Gomez-Hernandez and Gorelick, 1989; Dagan, 1990], leading to a greater appreciation of the effect of
503 spatial-scale effects on solute transport behavior [e.g., Gelhar et al., 1992; Neuman, 1990]. Driven by
504 some of these studies, the influence of soil heterogeneity on hillslope rainfall-runoff responses was also
505 explored [e.g. Binley et al., 1989; Merz and Plate, 1997].
506

A number of large-scale tracer experiments, for example at the Cape Cod site [LeBlanc et al., 1991] and the Borden site [Woodbury and Sudicky, 1991], provided new experimental insight into solute transport processes; however, the need for better tools to characterize heterogeneity at the field scale was evident. This was already recognized in the review of stochastic hydrology by Gelhar [1986], who commented: "*Future research should be directed to finding better methods of estimating input covariance parameters including improvements in statistical methodology as well as on indirect methods based on geophysical and geologic information or bulk hydraulic properties*". Following this recognition, the use of geophysics to aid characterization was indeed explored in some large-scale tracer transport studies. For the Canadian Twin Lake tracer tests [Moltyaner and Wills, 1991], over 5 km of GPR survey data were collected and used to support interpretation of borehole core logs to develop hydrostratigraphic profiles [Killey and Moltyaner, 1988]. Perhaps more significant, however, is the geophysical work conducted at the Macrodispersion Experiment (MADE) site in Columbus, Mississippi in the late 1980s. DC resistivity, EMI and SP surveys were conducted over the site with a view to determining geostatistical models that could relate to hydraulic conductivity variability through relatively simple, assumed, hydrogeophysical relationships. Although the EMI data proved ineffective, Rehfeldt et al. [1992] reported computed correlation lengths from the DC resistivity and SP data and compared these against those computed from more direct measures of hydraulic conductivity. This was the first study where geophysical data were used to infer statistical properties of the spatial structure of hydraulic properties, and this work no doubt helped to trigger greater interest in the use of geophysical data for quantitative subsurface characterization.

By the early 1990s several stochastic hydrology methods had been developed that helped provide information about the spatial structure of aquifer permeability given localized measurements of permeability (e.g. from core samples) and piezometric head data; however, most of these approaches were limited in a practical sense from the lack of data with a high spatial sampling density. Rubin et al. [1992] recognized the value of geophysical data to support such approaches and proposed a new Bayesian approach that used seismic data alongside traditional hydrology data to improve spatial models of permeability. Developments to their initial concepts using seismic data followed [Copty et al.,1993; Copty and Rubin, 1995], whilst Hubbard et al. [1997] explored the value of surface GPR surveys in recovering bimodal permeability structures in the vadose zone, assuming a link between permittivity and hydraulic conductivity. Also recognizing the potential of high-resolution GPR data for near-surface investigations, Rea and Knight [1998] explored the characteristics of GPR data in an attempt to

539 determine geostatistical properties of sedimentary structures, from which some relation to patterns in
540 permeability was assumed. Irving et al. [2009] later continued this work in their study of the correlation
541 structure of soil water content using high resolution GPR data. In the work of Hubbard et al. [1999] an
542 explicit framework for the computation of correlation structure information using geophysical data was
543 developed, exploiting the availability of new (cross-borehole) tomographic techniques. Building on the
544 Bayesian approach originally proposed by Rubin et al. [1992], Hubbard et al. [2001] demonstrated the
545 value of GPR and seismic data for the estimation of hydraulic conductivity distributions at the South
546 Oyster Bacterial Transport Site, using tracer test data for verification of estimated models. This study
547 took advantage of site-specific relationships between geophysical attributes and hydraulic conductivity
548 developed using co-located field measurements. In a study performed to quantify the value of different
549 types of data for constraining numerical flow and transport models based on different datasets collected
550 at the South Oyster study site, Scheibe and Chien [2003] found that conditioning to geophysical
551 interpretations with larger spatial support significantly improved the accuracy and precision of
552 subsurface model predictions, while conditioning to a large number of small-scale (borehole-based)
553 measurements did not significantly improve model predictions, and in some cases led to biased or
554 overly confident predictions.

555 Again with the goal of developing a model of the spatial variability of permeability, McKenna and Poeter
556 [1995] demonstrated how cross-well seismic tomography data can be used to identify hydrofacies,
557 which can help constrain a permeability inverse model based on hydraulic head data. The work of
558 Hyndman et al. [1994] and Hyndman and Gorelick [1996] followed a similar approach in that cross-
559 borehole seismic tomography data (Figure 8) were used to assign hydrofacies, but in these two studies
560 the permeability of each hydrofacies was inversely estimated from solute concentration measurements
561 from a tracer test. More recent examples demonstrating the use of geophysical data to develop
562 hydrofacies include Parra et al. [2006] and He et al. [2014].
563
564 INSERT FIGURE 8 NEAR HERE
565
566 Significant advances in characterizing hydrogeological heterogeneity using geophysical methods have
567 clearly been made. The field of hydrogeophysics has progressed from using geophysics in isolation to
568 approaches that attempt to honor multiple datatypes. In real problems, various data sources are likely
569 to exist and methodologies that can incorporate the breadth of data (with variable quality) are likely to
570 have practical value. Some approaches have focused on detailed mapping of hydraulic conductivity and

571 although such methods are likely to have value for problems at the site scale (e.g. in groundwater
572 cleanup operations), the approaches that extend to larger scales offer exciting potential. He et al.[2014],
573 for example, tackle structural characterization at the scale of multiple km^2 by using 3D maps of
574 electrical conductivity derived from airborne EM surveys along with borehole geological logs to develop
575 hydrofacies through a transitional probably framework (see Figure 9). Such methods account for
576 uncertainty within the hydrogeological model and are underpinned by geological reasoning, and may
577 lead to a new era of hydrogeological structural characterization at the large scale using geophysics.
578
579 INSERT FIGURE 9 NEAR HERE
580

581 Time – a new dimension for geophysical observations

582
583 Many of the early applications of geophysics to subsurface hydrology focused on structural
584 characterization using static geophysical data (as, for example, shown schematically in Figure 1). Limited
585 by the non-uniqueness of some geophysical – hydrological property relationships, many of these
586 investigations utilized geophysical measurements as 'soft' data, aiding in the identification of
587 hydrostratigraphy. However, it was soon realized that a number of geophysical properties are sensitive
588 to groundwater and soil states (moisture content, salinity, etc.) and thus a new avenue of research
589 developed, utilizing geophysical methods to explore temporal changes in states (see, for example, the
590 schematic in Figure 3). Those based on electrical conductivity or permittivity were initially explored as
591 some of the methodologies were reaching a level of maturity and the links between electrical
592 conductivity/permittivity and pore water composition and content were reasonably well understood.
593
594 Daily and Ramirez [1989] is one of the pioneering studies of time-lapse geophysical imaging. They
595 demonstrated the use of "electromagnetic geotomography" for monitoring changes in water content
596 due to heating of rock mass (used as a preliminary experiment for examining the changes in water
597 content in a nuclear repository setting). Their method is effectively cross-borehole low frequency GPR,
598 which senses variation in permittivity. The study of Daily et al. [1992] brought a major breakthrough in
599 hydrogeophysical investigation through their demonstration of a new technology, electrical resistivity
600 tomography (ERT), in cross borehole mode to examine the movement of a water tracer through the
601 vadose zone. They ran two field experiments (one lasting one day, the other lasting 72 days) and

602 demonstrated the capability of ERT for tracking the tracer movement (see Figure 10). Ramirez et al.
603 [1993] took this technology further by demonstrating its effectiveness in monitoring subsurface flow
604 pathways during steam injection for the remediation of hydrocarbon-contaminated groundwater, using
605 changes in electrical conductivity as a proxy for changes in temperature.
606
607 INSERT FIGURE 10 NEAR HERE
608
609 Other early time-lapse geophysical studies include that of Binley et al. [1996], who studied the
610 spatiotemporal changes in electrical conductivity (with ERT) in a large soil core during a tracer
611 experiment. Their results revealed a three-dimensional distribution of breakthrough curves, illustrating
612 preferential flow pathways. To illustrate the high spatiotemporal sampling of transport behavior they
613 coined the term “pixel breakthrough curves”, which was subsequently used in a number of time-lapse
614 hydrogeophysical studies. Zhou et al. [2001] also demonstrated the use of ERT for mapping preferential
615 flow, in this case in a small field plot. Eppstein and Dougherty [1998], Parkin et al. [2000], Binley et al.
616 [2001], Tsoflias et al. [2001], Alumbaugh et al. [2002] and Day-Lewis et al. [2003] are early examples of
617 the use of GPR for monitoring stimulated changes to the subsurface (e.g. tracer injection or well
618 pumping).
619
620 ERT and GPR techniques deal mostly with the production of 2D slices of the subsurface, or limited size
621 3D volumes. In comparison, EMI has proved useful in providing time-lapse images over relatively large
622 spatial areas. Although capable of providing semi-quantitative moisture maps [Huth and Poulton, 2007;
623 Robinson et al., 2012], especially when combined with point sensor data, the real strength in EMI is in
624 collecting qualitative data that identifies subsurface patterns of soil wetting and drying [Sherlock and
625 McDonnell, 2003; Robinson et al., 2009].
626
627 Most of these early examples served as demonstrations of techniques and provided only qualitative
628 interpretation of time-lapse geophysical signals. Binley et al. [2002] is one of the first attempts to use
629 time-lapse geophysical data from the field (in this case, cross borehole ERT and GPR) to calibrate a
630 hydrological model in a study of flow in an unsaturated sandstone. Kemna et al. [2002] and
631 Vanderborght et al. [2005] also showed how time-lapse geophysical data (ERT) could be used to help
632 quantify hydraulic properties. Kowalsky et al. [2005] also demonstrated the value of time-lapse
633 geophysical data for hydraulic parameter estimation. Several other studies have followed [e.g. Farmani

et al., 2008; Pollock and Cirpka, 2012; Camporese et al., 2012; Busch et al, 2013; Anh Phuong et al., 2014]. From this wide range of investigations, numerous approaches are now available for hydraulic parameter estimation using geophysics as a primary or secondary source of data.

Time-lapse geophysical imaging has also been effective in revealing new insight into subsurface flow and transport mechanisms. Singha et al. [2007], for example, showed how time-lapse electrical resistivity measurements can be used to characterize mass transfer in dual-porosity systems [see also Swanson et al., 2012; Briggs et al., 2013]. Slater et al. [2007] demonstrated the use of electrical conductivity monitoring for revealing biogenic gas development in peat, thus offering the potential to explore, at the field scale, the mechanisms of carbon-gas generation in peatland environments. Hayley et al. [2009], Strobach et al. [2014], and Van Dam et al. [2014], amongst others, have utilized time-lapse geophysical methods to reveal complex infiltration and shallow recharge processes, contributing to our understanding of field-scale processes.

The need to better understand the interaction of groundwater and surface water and the appreciation of the potential significance of biogeochemical processes that occur at the interface of groundwater and surface water (e.g. within the hyporheic zone) has encouraged the search for new ways of investigating this zone of interaction. Geophysical methods have provided some insight into the complexity of the architecture of the subsurface at this interface [e.g. Crook et al., 2008; Slater et al., 2010; Chambers et al.,2014]; however, time-lapse geophysical imaging has proved to be highly effective in mapping the dynamics of vertical and lateral exchange of flows under natural conditions [Christiansen et al., 2011; Ward et al., 2012; Meyerhoff et al., 2014] and due to anthropogenic induced events [Johnson et al., 2012; Wallin et al., 2013].

One issue with time-lapse data is the volume of data generated, and how to explore signals in those data effectively. One successful example of manipulating and parsing multiple large time-lapse data sets is that of Johnson et al.[2012], who focused on ways to extract relevant hydrological information using time-series analysis techniques applied to large datasets obtained from autonomous data collection systems. They utilized time-frequency analysis to identify relations between river stage and bulk electrical conductivity to understand the potential impacts of uranium transport in an aquifer connecting to the Columbia River (see Figure 11).

INSERT FIGURE 11 NEAR HERE

Such time-series analysis approaches offer one way of handling such large volumes of data; another is joint inversion of hydrologic and geophysical data (see earlier discussion on data inversion). Numerous techniques have evolved in recent years, including methods that focus on using tomograms themselves, which include the errors from inversion, to those based on hydrologic and geophysical data directly [e.g., Hyndman and Gorelick, 1996; Kowalsky et al., 2005; Looms et al.,2008]. Markov chain Monte Carlo methods are growing in popularity for jointly inverting hydrologic and geophysical data [Hinnell et al., 2010; Huisman et al., 2010; Irving and Singha, 2010; Laloy et al., 2012]. Such schemes offer future potential for parsing these large, complex hydrogeophysical data sets.

Biogeophysics: adding a biogeochemical dimension

As outlined above, early hydrogeophysical studies focused on characterizing the hydrogeological structure of the subsurface, in many cases motivated by the need to predict the fate of subsurface contaminants. Driven by the legacy of former industrial and military operations, some studies began to focus attention on using hydrogeophysical methods to assist in designing, and monitoring the effectiveness of, remediation techniques. Initially, these studies attempted to address the need for better understanding of subsurface heterogeneity in order to provide a hydrological structure in which the biogeochemical mechanisms could be assessed. The study by Hubbard et al. [2001] at the South Oyster Bacterial Transport Site is a key example of such work. Here, multiple geophysical techniques were used to develop a permeability model, with which the transport of bacteria injected into the site (for bioremediation) could be assessed.

It was soon realized that some geophysical measurements may offer additional value beyond describing the physical heterogeneity of the subsurface. Although both sediment physical and mineralogical properties play a critical role in controlling the geochemical and biogeochemical processes occurring in the subsurface, field studies typically acquire little or no mineralogical data. Because several geophysical attributes are influenced by sediment texture, and because mineralogy often co-varies with texture, geophysical methods can potentially be used to characterize mineralogy. As a first illustration of this concept, Chen et al. [2004] used a stochastic approach and GPR data to estimate subsurface ferric and ferrous iron distributions, estimates that were in turn used to improve reactive transport simulations of

698 redox-sensitive process at the South Oyster site [Scheibe et al., 2006]. The recent work of Sassen at al.
699 [2012] and Wainwright et al. [2014] developed and field tested a "reactive facies" concept focused on
700 using geophysical methods to characterize subsurface units having distinct and linked physicochemical
701 properties– a reactive transport equivalent (conceptually at least) to the much earlier hydrofacies
702 mapping of Hyndman et al. [1994], McKenna and Poeter [1995] and others (see Figure 12).
703
704 INSERT FIGURE 12 NEAR HERE
705
706 Geophysical surveys have also assisted in developing biogeochemical conceptual models at
707 contaminated sites, using, for example, electrical conductivity as a proxy for oxidation-reduction
708 processes [e.g. Lendvay et al., 1998]. The challenge is to use geophysical properties as indicators of
709 complex biogeochemical interactions at the field scale. Controlled laboratory experiments (e.g. as
710 reported in Williams et al [2005], Chen et al [2009], Regberg et al. [2011] and Revil et al. [2012b]) are
711 necessary to assess the value of geophysical measurements for quantifying biogeochemical processes
712 and products. Whereas electrical conductivity may remain an ambiguous measure for such purposes
713 (since it is controlled by physical and chemical states of the porous medium and its fluids), measures of
714 the electrical polarization of porous media have shown greater potential in the context of
715 biogeochemical characterization, given that these measures are more directly sensitive to grain/mineral
716 surface processes. For example, Williams et al. [2009] used time-lapse field IP data to infer
717 spatiotemporal variations in groundwater geochemistry due to microbial iron and sulfate reduction
718 induced through bioremediation and Vaudelet et al. [2011] illustrated the different electrical
719 polarization responses of silica sand with sorbed copper and sodium ions.
720
721 Despite the progress made, a reality check is prudent here to insure against unrealistic expectations of
722 geophysical measurements with respect to extractable information on biogeochemical processes. Many
723 biogeochemical processes involve a multitude of physical, chemical and/or biological transformations,
724 some of which may generate geophysical signatures [Atekwana and Atekwana, 2010]. Whereas it may
725 be possible to use time-series of geophysical data to ascertain when, where, and even how quickly
726 biogeochemical transformations are occurring, the complexity of these transformations limits the use of
727 geophysical measurements alone to quantify geochemical reactions involved or to quantify reliable
728 reaction rates at the field scale. However, recent developments have indicated how the integration of
729 time-lapse geophysical and aqueous geochemical datasets can be used to estimate the onset and

730 spatiotemporal distribution of biogeochemical transformations, including critical redox transitions [Chen
731 et al., 2009; 2013]. Similarly, although geophysical datasets may increasingly be used to highlight
732 hotspots of biogeochemical activity, for example associated with biodegraded contaminant plumes,
733 quantifying concentrations of microbes or aqueous/solid phase by-products of microbial activity from
734 geophysical observations is currently unlikely. However, laboratory electrical geophysical measurements
735 have been shown to produce time-lapse data that mimic the shape of classical bacterial growth curves
736 [Slater et al., 2009; Revil et al., 2012b], suggesting that characteristics of electrical datasets could be
737 used to infer some information on microbial growth rates (see Figure 13).
738
739 INSERT FIGURE 13 NEAR HERE
740

741 Applications to ecosystem science

742
743 Recognizing the two-way interaction between hydrological and ecological systems, many hydrological
744 investigations are nowadays linked to some ecosystem response; geophysics is suited to addressing such
745 issues and wider ecosystem questions [Jayawickreme et al., 2014]. For example, as nitrate
746 concentrations in an aquifer rise, recharge to a river or lake can have significant impact on the
747 ecosystems that depend on the surface water body. Similarly, as we strive to address the agricultural
748 demands of the planet, we must appreciate the subsurface water environment that crops (and hence
749 livestock) depend on [Sudduth et al., 2001]. Hydrogeophysical methods have evolved relatively recently
750 to address such ecohydrological problems.
751
752 Some key questions in ecohydrology include: What controls the spatial patterns of vegetation? How do
753 these spatial patterns influence local hydrology? How will hydrological and vegetation interactions
754 evolve with global change? How do these interactions influence the transfer of macronutrients to and
755 from the terrestrial environment? At the field and small catchment scale, addressing these questions
756 often presents a challenge because soil survey data often only provide qualitative information.
757
758 The work of Holden [2005] is an excellent early illustration of the value of hydrogeophysics for exploring
759 the link between surface vegetation species and piping in peatland catchments. He investigated the
760 occurrence of soil pipes in 160 UK peat catchments using a total of 115 km of GPR data. By

761 simultaneously mapping vegetation species in each plot, a link between *Calluna* species and soil pipe
762 occurrence was established that suggested that *Calluna* root development enhanced preferential flow in
763 these northern peatland environments.
764
765 EMI and electrical methods have also proved useful in addressing ecohydrological issues. EMI has been
766 used to investigate links between soil and vegetation spatial patterns in dryland ecosystems [Robinson
767 et al., 2008b; Robinson et al., 2010; Cassiani et al., 2012] and in the tropics [Brechet et al., 2012].
768 Recently, Franz et al. [2011] used EMI surveys of electrical conductivity to reveal how soil water patterns
769 are influenced by, and influence, vegetation in a Kenyan dryland environment (see Figure 14).
770 Frequency-domain, ground-based EMI methods were once considered primarily as reconnaissance tools
771 for qualitative mapping, however, there has been renewed interest given recent developments in multi-
772 coil instrumentation, which now offer the potential for rapid surveying of electrical conductivity at
773 multiple depths [e.g., Dafflon et al., 2013; Doolittle and Brevik, 2014; von Hebel et al., 2014].
774
775 INSERT FIGURE 14 NEAR HERE
776
777 DC resistivity has proved valuable for understanding soil moisture wetting patterns, redistribution, and
778 vegetation uptake. Jayawickreme et al. [2008] used it to monitor the influence of climate and vegetation
779 on root-zone soil moisture, bridging the intermediate scale gap between remotely-sensed and in-situ
780 point measurements. They went on to infer the hydrological consequences of land-cover change
781 [Jayawickreme et al., 2010]. The ability to penetrate to substantial depth allows for monitoring of deep
782 rooted trees which is infeasible using other methods. For example, Davidson et al. [2009] used DC
783 resistivity to study deep (> 11 m) rooting soil-water uptake in Amazonian woodlands during drought.
784 Moreover, the sensitivity to salinity allowed Jackson et al. [2005] to use it to show that the planting of
785 eucalyptus in shallow groundwater areas of Argentina had resulted in groundwater salinization. Other
786 recent examples illustrating how electrical methods can help with understanding ecohydrological
787 linkages include that of Comte et al. [2010], who showed, through electrical imaging of the subsurface,
788 how vegetation can influence the development of freshwater lenses in a small coral island. Befus et al.
789 [2013], in contrast, used electrical imaging to examine thermal buffering of intertidal zones by coastal
790 groundwater systems, and highlight the ecological significance of such processes for maintaining the
791 habitat of marine ecosystems.
792

793 Geophysical methods have also been used to study hydrological processes associated with managed
794 ecosystems, such as agricultural sites [Allred et al.,2008]. Examples include the use of soil moisture to
795 map vineyard water content and its influence on grapevine vigor [Lunt et al. 2005] and the joint use of
796 EMI and gamma-radiometric approaches to estimate cation exchange capacity and clay content in cereal
797 and sugarcane farms [Rodrigues et al., 2015]. Time-lapse geophysical monitoring has also been useful
798 for understanding the effectiveness of irrigation. For example, Michot et al. [2003] applied resistivity
799 imaging to monitor wetting patterns under irrigated corn (Figure 15); more recently, Garre et al. [2011]
800 illustrated the value of 3D resistivity imaging for improved understanding of root water uptake
801 processes. Geophysical techniques are also beginning to provide data to assist plant scientists in plant
802 breeding programs. Macleod et al. [2013] showed how ERT can support more conventional data types in
803 identifying grass hybrids that enhance soil structure and potentially alleviate flooding potential. More
804 recently, Shanahan et al. [2015] illustrated how EMI can help phenotype root function in wheat at the
805 field scale.
806
807 INSERT FIGURE 15 NEAR HERE
808
809 Complementing the ecohydrological studies described above, several studies have recently illustrated
810 the use of geophysical data to investigate hydrological and other controls on subsurface production of
811 greenhouse gasses, particularly in northern peatland and permafrost regions. Such improved
812 understanding of interactions between hydrological and biogeochemical processes occurring within
813 terrestrial ecosystems is required to reduce the uncertainty associated with global climate predictions
814 [Friedlingstein et al., 2014]. Terrestrial ecosystem feedbacks to climate can occur through a variety of
815 mechanisms, including through altering the energy balance, through vegetation dynamics, and through
816 microbial decomposition of soil organic carbon, which can release a large amount of carbon back into
817 the atmosphere as CO_2 and CH_4. Quantifying controls on greenhouse gas fluxes in terrestrial ecosystems
818 is challenging due to the wide range of interactions that occur in and across different compartments of
819 the ecosystem, including vegetation, land surface, and the subsurface.
820
821 A review of several studies given by Comas and Slater [2009] describes the use of GPR to characterize
822 the stratigraphy of peat systems and examine controls on CH_4 production dynamics in these systems,
823 including peat structure [Comas et al., 2014] and atmospheric pressure [Comas et al., 2011]. Permafrost
824 systems, which are vulnerable to climate change because large volumes of organic carbon are locked up

825 in the currently frozen but gradually warming permafrost, have also been a focus of recent
826 hydrogeophysical studies. In particular, geophysical methods have been used to characterize the nature
827 and distribution of properties within all compartments of these systems, including the permanently
828 frozen zone [e.g., Dou and Ajo-Franklin, 2014; Hauck et al., 2010] and the active layer [e.g., Brosten et
829 al., 2009]. A few new directions have emerged from these early studies that appear to be useful for
830 developing insights about how these complex systems function and for tractably providing information
831 over scales relevant for predicting ecosystem feedbacks. One is the use of airborne datasets to
832 characterize the spatial variability of specific compartments of the system over large spatial extents,
833 including permafrost using EMI [Minsley et al., 2012] and the active layer using LiDAR [Gangodagamage
834 et al., 2014]. The other is the coincident use of multiple above- and below- ground geophysical datasets
835 to characterize the co-variation of permafrost, active layer, and land-surface properties, and to use that
836 information to delineate functional zones in the landscape that have unique distributions of properties
837 that influence greenhouse gas fluxes [Hubbard et al., 2013].
838
839 The consideration of hydrogeophysical methods in ecosystem studies will no doubt continue to grow
840 because of the unique ability of hydrogeophysical measurements to provide spatially continuous
841 information on the shallow subsurface at the same landscape scale that is fundamental to
842 understanding many ecosystem processes. As already advocated by Robinson et al. [2008a], a top-down
843 multi-scale approach to ecosystem characterization seems ideal to make progress here. In such an
844 approach, joint semi-quantitative interpretation of multiple geophysical data can provide meaningful
845 delineations of landscape units that can be used to guide more detailed and quantitative site
846 investigations. Ideally, such an approach simultaneously provides the much needed spatial context to
847 local-scale investigations, and ensures that local-scale investigations are performed at representative
848 sites that capture landscape heterogeneity.
849
850 ## Future directions
851
852 Despite the significant developments in both theoretical and experimental aspects of hydrogeophysics,
853 as illustrated above, many challenges remain as we seek to better understand the subsurface
854 hydrological and biogeochemical processes, and their interaction with ecosystems. We highlight here a
855 number of areas worthy of future research within hydrogeophysics.

Watershed Systems: Key controls and characteristics

One of the key drivers for hydrogeophysics is the potential for mapping subsurface patterns over large areas. Much of the development to date, however, has been directed at plot-scale (i.e. tens of meters) experiments. Just as environmental regulators have established procedures for dealing with point source groundwater pollution but still struggle to manage diffuse source contamination, we have seen immense development of local-scale characterization in hydrogeophysics, but very little addressing problems at larger scales or beyond. For example, while cross-borehole methods may provide high-resolution information about geophysical properties, which may help quantify hydrological and biogeochemical parameters, they still have limited spatial extent. A few exemplars of large-scale mapping do exist, however, such as the aquifer mapping of Denmark, where successful attempts have been made to utilize ground-based and airborne geophysical surveys to aid the production of high resolution maps of aquifer bodies in order to develop reliable groundwater protection strategies [Thomsen et al., 2004]. We see an increasing trend in geophysical methodologies to characterize and monitor systems over watershed and landscape scales, or scales that are relevant to the management of systems for environmental remediation, water resources, agriculture, and carbon cycling challenges. We also anticipate an increasing trend in the strategic deployment of plot-scale experiments to reveal dominant mechanisms that have an impact at the larger scale, and to quantify hot spots (locations in space that exert an inordinate control on larger system behavior) and hot moments (sporadic periods in time associated with high levels of activity). In attempting to understand the transfer of macronutrients from terrestrial to freshwater environments, for example, it may be valid to focus attention along the zone of exchange (i.e. 'hot spots'), rather than in the entire watershed [e.g. Binley et al., 2013]. Furthermore, using geophysical techniques to help with the understanding of biogeochemical processing at the interface of groundwaters and surface waters (e.g. within the hyporheic zone) could be extremely beneficial to tackle the problems faced with managing diffuse pollution, particularly if such techniques can be applied over large scales.

Ubiquitous and Autonomous Environmental Sensing

The need to characterize over larger scales and monitor key dynamics with sufficient temporal resolution has been driving the development of new sensing approaches and platforms. For example, autonomous electrical resistivity tomographic methods are becoming commonly used for monitoring moisture content dynamics with high temporal and spatial resolution. Fiber-optic based distributed

888 temperature sensing methods [e.g., Selker et al., 2006] have recently enabled catchment hydrological
889 monitoring over greater scales of investigation and with significantly increased temporal and spatial
890 resolution relative to conventional approaches. Technological developments in Distributed Acoustic
891 Sensing (DAS) technologies emerging from the oil exploration industry [e.g. Mateeva et al., 2014], may
892 similarly enable improved characterization of subsurface systems, including permafrost dynamics. At
893 much larger scales, the opportunities presented by airborne methods become interesting. The study of
894 He et al.[2014] illustrated how electrical conductivity data obtained from an airborne platform can be
895 integrated into a stochastic geological modelling environment, covering an area of over 100 km^2 (see
896 Figure 9). Resolution of shallow (<10 m) structures is still relatively poor with such surveys, but the
897 technology is developing and improvements tailored to shallow mapping are emerging. Natural gamma
898 surveys are proving particularly useful for mapping mineral soils [Cook et al., 1996] and even soil organic
899 carbon (SOC). Rawlins et al. [2009] showed that the precision of regional predictions of SOC across
900 Northern Ireland was substantially improved by using auxiliary information on radiometric potassium
901 from airborne surveys. The challenges associated with both scale and cost of traditional airborne sensing
902 approaches are likely to be mitigated by the rapid development of unmanned land and aerial vehicles. In
903 particular, technological innovations associated with unmanned aerial vehicles (UAVs) (which are
904 allowing longer flight times, multiple sensor payloads, and cheaper cost) are expected to greatly
905 accelerate the ability to monitor natural environments.
906
907 ***Data fusion and assimilation***
908 The majority of hydrogeophysical applications to date have focused on single modality datasets (i.e. one
909 geophysical measurement approach). Combining multiple single modality surveys is relatively
910 straightforward and thus 'stitching' datasets to form composite datasets covering a large area is
911 achievable. However, in many cases we may be armed with data from multiple modalities, measuring
912 different properties, in different configurations, with different depths of investigation and measurement
913 support volume (e.g. Figure 5). Rather than treating each dataset independently, we should endeavor to
914 formulate a single coherent image (model) of the subsurface. Coupled hydrogeophysical inversion
915 approaches, as discussed earlier, go some way towards achieving this goal, but no generalized approach
916 currently exists and more work is needed to provide practical solutions that do not depend on
917 substantial *a priori* knowledge of the subsurface.
918
919 ***Uncertainty and information***

Uncertainty in hydrological models is now well established and yet most hydrogeophysical studies fail to recognize uncertainty in geophysical models and the transfer of these to hydrology. The treatment of measurement and model uncertainty in geophysics is not new, and yet it is routinely ignored. Such failure to account for uncertainty can incorrectly portray accuracy and resolution and can lead to misleading interpretation. The computational burden of computing some form of uncertainty estimate in an inversion is probably the main cause of such failure, however, for many plot-scale 2D studies computational demands should not preclude some assessment of model uncertainty. Uncertainty in model interpretation also propagates through from any constitutive relationships linking geophysical and hydrological properties, and yet these relationships are frequently assumed to be precise and error free. Greater recognition of all the contributing sources of uncertainty is needed in future studies. It may be that in some cases, geophysical data can provide little improvement over *a priori* estimates of some hydrological (or biogeochemical) quantity. Declaration of this limitation will not undermine hydrogeophysics.

Related to uncertainty estimation, there has also been a distinct lack of analysis of information content (or data worth) in the majority of hydrogeophysical studies. As we invest more resources for subsurface investigation it may be appropriate, in some studies, to question the worth of data during the survey design stage. JafarGandomi and Binley [2013] recently examined the information content of different geophysical data modalities using a simple Shannon Entropy measure in a Bayesian data fusion framework. One can envisage using cost functions in such an approach to deliver a realistic cost-benefit analysis of different geophysical data types.

N=1 experimentation

As in other areas of field-based experimental hydrology, we are often challenged with a sample size of one (a single hillslope, watershed, etc.). Consequently, in comparison to other science disciplines, our observations may be perceived to be anecdotal. For example, revealing preferential flow through soils in one small field plot does not necessarily demonstrate that such a phenomenon is prevalent across an entire watershed. However, there are opportunities, in some cases, for more robust experimental design that can help strengthen the value of hydrogeophysics. Where possible, comparisons against controls are needed along with more replicate studies. In a recent study, for example, Shanahan et al. [2015] used time-lapse EMI measurements on plots each sown with one of 23 breeds of wheat, each with four replicates in a random block experimental design, to demonstrate that different breeds extract

952 water from different depths of soil. Such experimental design may not be appropriate for many
953 hydrogeophysical applications, but where applicable they can help steer hypothesis-driven research. The
954 failure to use replicates in laboratory experiments is a clear weakness of many studies of the
955 relationships between geophysical and hydrological properties.
956
957 ***Emerging application areas***
958 We have illustrated throughout this paper the progression of hydrogeophysics from tools for structural
959 characterization to a means of studying the dynamics of subsurface hydrological and biogeochemical
960 processes, and branching out to ecosystem science. We anticipate greater exploitation of geophysics for
961 studying both natural and managed ecosystems. For example, as the need to produce more food with
962 less resources (fertile land, fertilizer, water) increases, there is a significant opportunity to use
963 geophysical approaches to advance precision farming and plant breeding programs. The plant sciences
964 literature is beginning to show recognition of the potential value of geophysical methods in a wide range
965 of areas, such as ERT and SP for monitoring root function and biomass [Amato et al., 2009; Li et al.,
966 2015], and mapping root architecture with GPR [Hirano et al., 2012]. In his discussion on ecohydrology,
967 van Dijk [2004] argued that: "*to date, no consistent physical theory has been developed to describe the*
968 *relationships between topography, ecosystem maintenance and modification of soil structure, and the*
969 *alteration of soil hydraulic properties all of which contribute to the expression of plant community*
970 *structure, and are fundamental to understanding the long-term impacts of climate and land-use*
971 *change*". As previously described, geophysical approaches are now being developed to study the
972 interactions and feedbacks between different compartments of terrestrial environments, with recent
973 examples in peatland and permafrost ecosystems that are particularly vulnerable to climate change.
974 New trends, such as the use of above-and-below ground sensing approaches and the identification of
975 ecosystem functional zones [Hubbard et al., 2013] are expected to provide insights about how terrestrial
976 environments are responding to climate and land-use associated stresses, and the associated
977 implications for ecosystem services, including food production, clean water availability, and carbon
978 sequestration.
979
980
981 ## Closing remarks
982

As illustrated with the examples reported here, the past 25 years have seen an immense growth in the development of new geophysical measurement approaches (and customization of existing methods) for investigating the subsurface environment. We have now developed greater insight into the sensitivity of geophysical parameters to processes that control the hydrological, biogeochemical and ecological functioning of the subsurface and interactions with non-terrestrial environments. The numerous works published in *Water Resources Research* and many other journals and texts illustrate how hydrogeophysics has emerged as an established sub-discipline of hydrology, with strong connections to many other fields, such as biogeochemistry, ecology, near surface geophysics, etc. The field is growing rapidly as emerging technologies (instruments, models) and new insights into hydrogeophysical relationships open up new areas for research and potential solutions to significant and challenging environmental problems.

Figure and table captions

Figure 1. Cartoon of a terrestrial environment, illustrating hydrogeological heterogeneity and how geophysical methods are often used to characterize the 'hidden' subsurface. Geophysical datasets provide information about geophysical properties, such as electrical conductivity (shown here), which can potentially be related to hydrogeological properties as shown in Table 1.

Figure 2. (a) Number of hydrogeophysics – related papers published per year in *Water Resources Research* since 1990. (b) Number of hydrogeophysics – related papers expressed as a percentage of total published papers per year in *Water Resources Research* (Source: ISI Web of Science).

Figure 3. Schematic representation of geophysical data inversion. The region of interest is investigated through the measurement of responses to signal sources recorded on a number of receiver sensors. The region is discretized into a series of geophysical model parameters (m) that are consistent with the data (d) through some inverse function (G^{-1}). Changes in subsurface states are shown in the left figure at different times (T_0, T_1, T_2), which may represent evolution of a remediation process or contaminant plume. The geophysical image on the right represents a snapshot of the distribution of a geophysical property at a particular time.

Figure 4. Example joint inversion of cross well ERT and GPR data in the unsaturated zone of a sandstone aquifer, modified after Linde et al. [2006]. The 3D volume contains regions where electrical conductivity (from cross-well ERT) and relative permittivity (from cross-well GPR) follow different joint relationships, which Linde et al.[2006] quantified to propose four lithological units.

Figure 5. Comparison of horizontal and vertical survey scales typically achievable in one day by a two person field crew for ERT, FDEM and TDEM. ERT(1) and ERT(5) refer to 1m and 5m spaced electrode arrays, respectively. FDEM(1) and FDEM(3.5) refer to 1m coil and 3.5m coil instruments, respectively. For TDEM we assume a 50m loop sounding at multiple stations along a transect.

Figure 6. Illustration of hydrogeophysical relationships in porous media. The blue arrows represent electrical pathways at the pore scale. At some representative volume, the macroscopic measurement of electrical conductivity (EC) is linked to some property (e.g. porosity) or state (e.g. fluid saturation).

Figure 7. Comparison of permeability (k) modeled from SIP measurements of an electrical time constant (τ_p) or relaxation frequency (f_p) and measured permeability [modified from Revil, 2013].Here, $D_{(+)}^{S}$ is the diffusion coefficient of cations in the Stern layer of the electrical double layer, and F is the formation factor.

Figure 8. Distribution of seismic slowness at the Kesterton site, modified after Hyndman and Gorelick [1996]. The 3D distribution represents a realization of slowness generated using sequential Gaussian simulation, preserving the correlation lengths and probability distributions from cross-well seismic tomograms obtained within the boxed region in the image. Hyndman and Gorelick [1996] used this information along with observations from tracer tests to compute 3D images of the zonation of hydraulic conductivity at the site.

Figure 9. Simulated probabilities of sand fraction at a specific depth based on transitional probabilities conditioned on different data, modified after He et al. [2014]. The left image shows probabilities conditioned on borehole data (locations shown as dots in the image). The right image shows probabilities conditioned on borehole data and electrical conductivity obtained using airborne EMI. The black line shows the boundary of the geophysical survey. Each rectangular image represents an area of

1046 108 km^2. He et al. [2014] demonstrate the value of adding the geophysical data to this structural
1047 characterization problem.
1048
1049 Figure 10. Tracking the migration of a water tracer injected in the vadose zone using cross-well ERT,
1050 modified after Daily et al. [1992]. The images show change in resistivity at different times after injection
1051 of the tracer. The two long vertical lines indicate the 17.3m deep boreholes (positioned 7.4m apart). The
1052 tracer was injected in the central 4m deep borehole (also shown). Cooler colors represent a decrease in
1053 resistivity (associated with an increase in water content). The tracer injection stopped after 150 minutes.
1054
1055 Figure 11. Time series analysis of ERT data, modified after Johnson et al. [2012]. The images show the
1056 correlation between the temporal variation in river stage and observed changes in subsurface electrical
1057 conductivity. The river is on the eastern edge of the imaged region. Each image is a horizontal slice at
1058 different elevations through the 3D volume. The horizontal slice at 98m highlights the localized area of
1059 temporal changes in electrical conductivity that appear strongly linked to river stage change.
1060
1061 Figure 12. Reactive facies-based transport properties along the centerline of the uranium-contaminated
1062 Savanah River Site F-Area plume, modified after Wainwright et al. [2014]. Stochastic approaches were
1063 used to integrate multi-scale, multi-type measurements (including surface seismic data), providing
1064 estimates of hydrological and mineralogical properties important for controlling plume behavior to a
1065 reactive transport model - in high resolution and over plume-relevant spatial extents. The upper image
1066 shows estimated percent fines; the middle image shows hydraulic conductivity (log_{10} cm/s); the lower
1067 image shows Al-Fe ratios.
1068
1069 Figure 13. Modeled and measured change in quadrature electrical conductivity (from IP) during bacterial
1070 growth, modified after Revil et al.[2012].
1071
1072 Figure 14. Electrical conductivity maps obtained from EMI surveys at a Kenyan dryland site, modified
1073 after Franz et al. [2011], showing electrical conductivity variations over time, reflecting moisture content
1074 changes in patches of *Sansevieria volkensii* following a 6mm rainfall even on 24/25 July 2009. The blue
1075 boundaries indicate surface run-on zones; red boundaries show surface runoff zones. More noticeable
1076 changes in electrical conductivity, and hence soil moisture, occur inside the *S. volkensii* patches than in

the interpatch areas. Franz et al. [2011] hypothesized this to be due to low infiltration within the interpatches, coupled with capture of run-on and increased infiltration in the *S. volkensii* patches.

Figure 15. Changes in soil water content derived from ERT images, during irrigation of a corn crop, modified after Michot et al. [2003]. Thirty two electrodes were placed at 0.2m spacing along the ground surface. The images show changes in soil water content inferred from changes in resistivity.

TABLE 1: List of commonly used geophysical methods in hydrology and the geophysical properties they sense.

References

Abaza, M. M., and C. G. Clyde (1969), Evaluation of the rate of flow through porous media using electrokinetic phenomena, *Water Resour. Res.*, **5**(2), 470–483.

Ahmed, A. S., A. Jardani, A. Revil, and J. P. Dupont (2014), Hydraulic conductivity field characterization from the joint inversion of hydraulic heads and self- potential data, *Water Resour. Res.*, **50**(4), 3502-3522,DOI:10.1002/2013wr014645.

Allred, B., J. J. Daniels, M. R. Ehsani, 2008, *Handbook of Agricultural Geophysics*, CRC Press, 432pp.

Alumbaugh, D., P. Y. Chang, L. Paprocki, J. R. Brainard, R. J. Glass and C. A. Rautman (2002), Estimating moisture contents in the vadose zone using cross-borehole ground penetrating radar: A study of accuracy and repeatability. *Water Resour. Res.,* **38**, 1309, DOI: 1310.1029/2001/WR000754.

Amato, M., G. Bitella , Roberta Rossi, J.A. Gómez, S. Lovelli, and J. J. Ferreira Gomes (2009), Multi-electrode 3D resistivity imaging of alfalfa root zone, *Europ. J. Agronomy*, **31**, 213–222, DOI:10.1016/j.eja.2009.08.005.

André, F., C. van Leeuwen, S. Saussez, R. Van Durmen, P. Bogaert, D. Moghadas, L. de Rességuier, B. Delvaux, H. Vereecken and S. Lambot (2012), High-resolution imaging of a vineyard in south of France using ground-penetrating radar, electromagnetic induction and electrical resistivity tomography. *Journal of Applied Geophysics*, **78**, 113-122.

1107 Anh Phuong, T., M. Vanclooster, M. Zupanski, and S. Lambot (2014), Joint estimation of soil moisture
1108 profile and hydraulic parameters by ground- penetrating radar data assimilation with
1109 maximum likelihood ensemble filter, *Water Resour. Res.*, **50**(4), 3131-3146,
1110 DOI:10.1002/2013wr014583.
1111 Archie, G.E. (1942), The electrical resistivity log as an aid in determining some reservoir characteristics.
1112 *Transactions of the American Institute of Mining, Metallurgical and Petroleum Engineers*,
1113 **146**, 54-62.
1114 Atekwana, E.A., and E.A. Atekwana (2010), Geophysical Signatures of Microbial Activity at Hydrocarbon
1115 Contaminated Sites: A Review, *Surv. Geophys.*, **31**, 247–283
1116 Auken, E., and A. V. Christiansen (2004), Layered and laterally constrained 2D inversion of resistivity
1117 data, *Geophysics*, **69**(3), 752-761,DOI:10.1190/1.1759461.
1118 Befus, K. M., M. B. Cardenas, D. V. Erler, I. R. Santos, and B. D. Eyre (2013), Heat transport dynamics at a
1119 sandy intertidal zone, *Water Resour. Res.*, **49**(6), 3770-3786, DOI:10.1002/wrcr.20325.
1120 Binley, A., J. Elgy and K. Beven (1989), A physically based model of heterogenous hillslopes 2. Effective
1121 hydraulic conductivities, *Water Resour. Res.*, **25**(6), 1227-
1122 1233,DOI:10.1029/WR025i006p01227.
1123 Binley, A., S. Henry-Poulter and B. Shaw (1996), Examination of solute transport in an undisturbed soil
1124 column using electrical resistance tomography, *Water Resour. Res.*, **32**, 763-769.
1125 Binley, A., P. Winship, R. Middleton, M. Pokar and J. West (2001), High-resolution characterization of
1126 vadose zone dynamics using cross-borehole radar, *Water Resour. Res.*, **37**, 2639-2652.
1127 Binley, A., G. Cassiani, R. Middleton and P. Winship (2002), Vadose zone flow model parameterisation
1128 using cross-borehole radar and resistivity imaging, *Journal of Hydrology*, **267**, 147-159.
1129 Binley, A., L. D. Slater, M. Fukes and G. Cassiani (2005), Relationship between spectral induced
1130 polarization and hydraulic properties of saturated and unsaturated sandstone, *Water*
1131 *Resour. Res.*, **41**, W12417,DOI:12410.11029/12005WR004202.
1132 Binley, A., S. Ullah, A. L. Heathwaite, C. Heppell, P. Byrne, K. Lansdown, M. Trimmer, and H. Zhang
1133 (2013), Revealing the spatial variability of water fluxes at the groundwater-surface water
1134 interface, *Water Resour. Res.*, **49**(7), 3978-3992,DOI:10.1002/wrcr.20214.
1135 Blainey, J. B., T. P. A. Ferré, and J. T. Cordova (2007), Assessing the likely value of gravity and drawdown
1136 measurements to constrain estimates of hydraulic conductivity and specific yield during
1137 unconfined aquifer testing, *Water Resour. Res.*, 43, W12408, doi:10.1029/ 2006WR005678.

1138 Bréchet, L., M. Oatham, M. Wuddivira, and D.A. Robinson (2012), Determining Spatial Variation in Soil
1139 Properties in Teak and Native Tropical Forest Plots Using Electromagnetic-Induction.
1140 *Vadose Zone Journal*. **11**(4), DOI:10.2136/vzj2011.0102.
1141 Briggs, M. A., F. D. Day-Lewis, J. B. T. Ong, G. P. Curtis, and J. W. Lane Simultaneous estimation of local-
1142 scale and flow path-scale dual-domain mass transfer parameters using geoelectrical
1143 monitoring, *Water Resour. Res.*, **49**(9), 5615-5630, doi:10.1002/wrcr.20397.
1144 Brosten, T.R., J.H. Bradford, J.P. McNamara, M.N. Gooseff, J.P. Zarneske, W.B. Bowden and M.E.
1145 Johnston (2009), Estimating 3D variation in active layer thickness beneath arctic streams
1146 using ground penetrating radar, *Journal of Hydrology*, **373**, 479-486.
1147 Brovelli, A., and G. Cassiani (2011), Combined estimation of effective electrical conductivity and
1148 permittivity for soil monitoring, *Water Resour. Res.*, **47**, W08510,
1149 DOI:10.1029/2011wr010487.
1150 Brovelli, A., G. Cassiani, E. Dalla, F. Bergamini, D. Pitea, and A. M. Binley (2005), Electrical properties of
1151 partially saturated sandstones: Novel computational approach with hydrogeophysical
1152 applications, *Water Resour. Res.*, **41**(8), W08411,DOI: 10.1029/2004wr003628.
1153 Busch, S., L. Weihermueller, J. A. Huisman, C. M. Steelman, A. L. Endres, H. Vereecken, and J. van der
1154 Kruk (2013), Coupled hydrogeophysical inversion of time-lapse surface GPR data to
1155 estimate hydraulic properties of a layered subsurface, *Water Resour. Res.*, **49**(12), 8480-
1156 8494,DOI:10.1002/2013wr013992.
1157 Camporese, M., G. Cassiani, R. Deiana and P. Salandin (2012), Assessment of local hydraulic properties
1158 from electrical resistivity tomography monitoring of a three-dimensional synthetic tracer
1159 test experiment, *Water Resour. Res.*, **47**. DOI: 10.1029/2011wr010528.
1160 Cassiani, G., N. Ursino, R. Deiana, G. Vignoli, J. Boaga, M. Rossi, M. T. Perri, M. Blaschek, R. Duttmann, S.
1161 Meyer, R. Ludwig, A. Soddu, P. Dietrich and U. Werban (2012), Noninvasive Monitoring of
1162 Soil Static Characteristics and Dynamic States: A Case Study Highlighting Vegetation Effects
1163 on Agricultural Land, *Vadose Zone Journal*, **11**. DOI: 10.2136/Vzj2011.0195.
1164 Chambers, J. E., P. B. Wilkinson, S. Uhlemann, J. P. R. Sorensen, C. Roberts, A. J. Newell, W. O. C. Ward,
1165 A. Binley, P. J. Williams, D. C. Gooddy, G. Old, and L. Bai (2014), Derivation of lowland
1166 riparian wetland deposit architecture using geophysical image analysis and interface
1167 detection, *Water Resour. Res.*, **50**(7), 5886-5905,DOI:10.1002/2014wr015643.

1168 Chan, C. Y., and R. J. Knight (1999), Determining water content and saturation from dielectric
1169 measurements in layered materials, *Water Resour. Res.*, **35**(1), 85-
1170 93,DOI:10.1029/1998wr900039.
1171 Chelidze, T.L. and Y. Gueguen (1999), Electrical spectroscopy of porous rocks: a review—I.Theoretical
1172 models, *Geophys. J. Int.*, **137**(1), 1-15.
1173 Chen, J., S. Hubbard, Y. Rubin, C. Murray, E. Roden and E. Majer, (2004), geochemical characterization
1174 sing geophysical data and Markov Chain Monte Carol methods: A case study at the South
1175 Oyster bacterial transport site in Virginia, *Water Resour. Res.*, **40**, W12412.
1176 Chen, J., S. S. Hubbard, K. H. Williams, S. Pride, L. Li, C. Steefel and L. Slater (2009), A state-space
1177 Bayesian framework for estimating biogeochemical transformations using time-lapse
1178 geophysical data, *Water Resour. Res*., **45**, W08420, DOI:08410.01029/02008WR007698.
1179 Chen, J., S.S. Hubbard, K.H. Williams (2013), Data-driven approach to identify field-scale biogeochemical
1180 transitions using geochemical and geophysical data and hidden Markov models:
1181 Development and application at a uranium-contaminated aquifer, *Water Resour. Res*, **49**,
1182 DOI 10.1002/wrcr.20524.
1183 Chen, Y., and D. Or (2006), Geometrical factors and interfacial processes affecting complex dielectric
1184 permittivity of partially saturated porous media*, Water Resour. Res*., **42**(6),
1185 W06423,DOI:10.1029/2005wr004744.
1186 Christensen, N.B. and K. Sørensen (2001), Pulled array continuous electrical sounding with an additional
1187 inductive source: an experimental design study, *Geophysical Prospecting*, **49**, 241-254.
1188 Christiansen, P. J. Binning, D. Rosbjerg, O. B. Andersen and P. Bauer-Gottwein (2011), Using time-lapse
1189 gravity for groundwater model calibration: An application to alluvial aquifer storage, *Water*
1190 *Resour. Res.,* **47**, DOI: 10.1029/2010wr009859.
1191 Comas, X., and L. Slater (2007), Evolution of biogenic gases in peat blocks inferred from noninvasive
1192 dielectric permittivity measurements, *Water Resour. Res.,* **43**(5),
1193 W05424,DOI:10.1029/2006wr005562.
1194 Comas, X., and L. Slater (2009), Non-invasive field-scale characterization of gaseous-phase methane
1195 dynamics in peatlands using the ground penetrating radar (GPR) method, in *Carbon Cycling*
1196 *in Northern Peatlands*, edited by A. Baird et al., 159-172, AGU, Washington, D.C.
1197 Comas, X., Slater, L., and Reeve, A. (2011), Atmospheric Pressure Drives Changes in the Vertical
1198 Distribution of Biogenic Free-Phase Gasses in a Northern Peatland. *Journal of Geophysical*
1199 *Research-Biogeosciences*, **116**, G04014, DOI:10.1029/2011JG001701

Comas, X., N. Kettridge, A. Binley, L. Slater, A. Parsekian, A.J. Baird, M. Strack, and J.M. Waddington (2014), The effect of peat structure on the spatial distribution of biogenic gases within bogs, *Hydrological Processes*, **28**(22), DOI: 10.1002/hyp.10056.

Comte, O. Banton, J.-L. Join and G. Cabioch (2010), Evaluation of effective groundwater recharge of freshwater lens in small islands by the combined modeling of geoelectrical data and water heads, *Water Resour. Res.*, **46**, DOI: 10.1029/2009wr008058.

Constable, S.C., R. L. Parker and C. G. Constable (1987), Occam's inversion: a practical algorithm for generating smooth models from electromagnetic sounding data. *Geophysics*, **52**, 289-300.

Cook, P. G., and S. Kilty (1992), A helicopter-borne electromagnetic survey to delineate groundwater recharge rates, *Water Resour. Res.*, 28(11), 2953-2961,DOI:10.1029/92wr01560.

Cook, S.E., R.J. Corner, P.R. Groves, and G.J. Grealish (1996), Use of airborne gamma radiometric data for soil mapping, *Australian Journal of Soil Research*, **34**, 183–194.

Copty, N., and Y. Rubin (1995), A stochastic approach to the characterization of lithofacies from seismic and well data, *Water Resour. Res.*, **31**(7), 1673-1686,DOI:10.1029/95wr00947.

Copty, N., Y. Rubin and G. Mavko (1993), Geophysical-hydrological identification of field permeabilities through Bayesian updating. *Water Resour. Res.*, **29**, 2813-2825.

Costabel, S., and U. Yaramanci (2013), Estimation of water retention parameters from nuclear magnetic resonance relaxation time distributions, *Water Resour. Res*., 49(4), 2068-2079,DOI:10.1002/wrcr.20207.

Crook, N., A. Binley, R. Knight, D. A. Robinson, J. Zarnetske and R. Haggerty (2008), Electrical resistivity imaging of the architecture of substream sediments, *Water Resour. Res*., **44**, DOI: W00D13, 10.1029/2008wr006968.

Cuma, M. and M.S. Zhdanov (2014), Massively parallel regularized 3D inversion of potential fields on CPUs and GPUs, 2014, *Computers & Geosciences*, **62**, 80–87.

Dagan, G. (1990), Transport in heterogeneous porous formations – spatial moments, ergodicity, and effective dispersion, *Water Resour. Res.*, **26**(6), 1281-1290, DOI:10.1029/WR026i006p01281.

Daily, W., and A. Ramirez (1989), Evaluation of electromagnetic tomography to map insitu water in heated welded tuff, *Water Resour. Res.*, **25**(6), 1083-1096, DOI:10.1029/WR025i006p01083.

Daily, W., and E. Owen (1991), Cross-borehole resistivity tomography, *Geophysics*, **56**,1228-1235.Daily, W., A. Ramirez, D. LaBrecque and J. Nitao (1992), Electrical resistivity tomography of vadose water movement. *Water Resour. Res*., **28**, 1429-1442.

1232 Dafflon, B.S.S. Hubbard, C. Ulrich and J.E. Peterson (2013), Electrical conductivity imaging of active layer
1233 and permafrost in an Arctic Ecosystem, through advanced inversion of electromagnetic
1234 induction data, *Vadose Zone Journal*, DOI 10.2136/vzj2012.0161.
1235 Darnet, M., G. Marquis, P. Sailhac (2003), Estimating aquifer hydraulic properties from the inversion of
1236 surface Streaming Potential (SP) anomalies. *Geophysical Research Letters*, **30**, 1679.
1237 Davidson E., P.A. Lefebvre, P.M. Brando, D.M. Ray, S.E. Trumbore, L.A. Solorzano, J.N. Ferreira, M.M.D.
1238 Bustamante and D.C. Nepstad (2009), Carbon inputs and water uptake in deep soils of an
1239 eastern Amazon forest. *Forest Science,* **57**, 51–58.
1240 Davis, K. and L. Li (2011), Fast solution of geophysical inversion using adaptive mesh, space-filling curves
1241 and wavelet compression, *Geophys. J. Int.,* **185**, 157–166, DOI: 10.1111/j.1365-
1242 246X.2011.04929.x.
1243 Day-Lewis, F.D., J. W. Lane, J. M. Harris and S. M. Gorelick (2003), Time-lapse imaging of saline-tracer
1244 transport in fractured rock using difference-attenuation radar tomography, *Water Resour.*
1245 *Res*., **39**, 1290, DOI: 1210.1029/2002WR0011722.d
1246 Day-Lewis, F. D., Y. Chen, and K. Singha (2007), Moment inference from tomograms, *Geophys. Res. Lett.*,
1247 **34**, L22404, doi:10.1029/2007GL031621.
1248 Dlubac, K., R. Knight, Y.-Q. Song, N. Bachman, B. Grau, J. Cannia, and J. Williams (2013), Use of NMR
1249 logging to obtain estimates of hydraulic conductivity in the High Plains aquifer, Nebraska,
1250 USA, *Water Resour. Res*., **49**(4), 1871-1886,DOI:10.1002/wrcr.20151.
1251 Doolittle, J.A and E.C. Brevik (2014), The use of electromagnetic induction techniques in soil studies,
1252 *Geoderma*, 223-225, 33-45.
1253 Dorn, C., N. Linde, T. Le Borgne, O. Bour, and L. Baron (2011), Single-hole GPR reflection imaging of
1254 solute transport in a granitic aquifer, *Geophys. Res. Lett.*, **38**, L08401,
1255 doi:10.1029/2011GL047152.
1256 Dou, S., and J. Ajo-Franklin (2014), Full-wavefield inversion of surface waves for mapping embedded
1257 low-velocity zones in permafrost, *Geophysics*, **79**(6), EN107-EN124, DOI:10.1190/geo2013-
1258 0427.
1259 Doussan, C., and S. Ruy (2009), Prediction of unsaturated soil hydraulic conductivity with electrical
1260 conductivity, *Water Resour. Res*., **45**, W10408,DOI:10.1029/2008wr007309.
1261 Eppstein, M. J., and D. E. Dougherty (1998), Efficient three-dimensional data inversion: Soil
1262 characterization and moisture monitoring from cross-well ground-penetrating radar at a
1263 Vermont test site, *Water Resour. Res*., **34**(8), 1889-1900,DOI:10.1029/98wr00776.

1264 Farmani, M. B., N.-O. Kitterod, and H. Keers (2008), Inverse modeling of unsaturated flow parameters
1265 using dynamic geological structure conditioned by GPR tomography, *Water Resour. Res.*,
1266 **44**(8), W08401,DOI:10.1029/2007wr006251.
1267 Feng, W., M. Zhong, J. M. Lemoine, R. Biancale, H. T. Hsu, and J. Xia (2013), Evaluation of groundwater
1268 depletion in North China using the Gravity Recovery and Climate Experiment (GRACE) data
1269 and ground-based measurements, *Water Resour. Res.*, **49**(4), 2110-2118,
1270 DOI:10.1002/wrcr.20192.
1271 Franz, T. E., E. G. King, K. K. Caylor, and D. A. Robinson (2011), Coupling vegetation organization patterns
1272 to soil resource heterogeneity in a central Kenyan dryland using geophysical imagery, *Water*
1273 *Resour. Res.,* **47**, W07531, DOI:10.1029/2010wr010127.
1274 Friedlingstein, P., M. Meinshausen, V. K. Arora, C. D. Jones, A. Anav, S. K. Liddicoat, and R. Knutti, (2014),
1275 Uncertainties in CMIP5 Climate Projections due to Carbon Cycle Feedbacks. *J. Climate*, **27**,
1276 511–526.
1277 Friedman, S. P., and D. A. Robinson (2002), Particle shape characterization using angle of repose
1278 measurements for predicting the effective permittivity and electrical conductivity of
1279 saturated granular media, *Water Resour. Res.,* **38**(11), 1236,DOI:10.1029/2001wr000746.
1280 Gallardo, L. A., and M. A. Meju (2003), Characterization of heterogeneous near-surface materials by joint
1281 2-D inversion of dc resistivity and seismic data, *Geophys. Res. Lett*., **30**(13), 1658,
1282 DOI:10.1029/2003GL017370.
1283 Gallardo, L. A., and M. A. Meju (2011), Structure-coupled multiphysics imaging in geophysical sciences,
1284 *Rev. Geophys*., **49**, RG1003, DOI:10.1029/2010RG000330.
1285 Gangodagamage, C., J. C. Rowland, S. S. Hubbard, S. P. Brumby, A. K. Liljedahl, H. Wainwright, C. J.
1286 Wilson, G. L. Altmann, B. Dafflon, J. Peterson, C. Ulrich, C. E. Tweedie, and S. D.
1287 Wullschleger (2014), Extrapolating active layer thickness measurements across Arctic
1288 polygonal terrain using LiDAR and NDVI data sets, *Water Resour. Res*., 1944-7973,
1289 DOI:10.1002/2013WR014283
1290 Garré, S., M. Javaux, J. Vanderborght, L. Pagès, and H. Vereecken (2011), Three-dimensional electrical
1291 resistivity tomography to monitor root zone water dynamics. *Vadose Zone Journal*, **10**, 412-
1292 424.
1293 Gehman, C. L., D. L. Harry, W. E. Sanford, J. D. Stednick, and N. A. Beckman (2009), Estimating specific
1294 yield and storage change in an unconfined aquifer using temporal gravity surveys, *Water*
1295 *Resour. Res*., 45, W00D21, doi:10.1029/2007WR006096.

1296 Gelhar, L.W. (1986), Stochastic subsurface hydrology from theory to applications. *Water Resour. Res.*,
1297 **22**, 135S-145S.
1298 Gelhar L.W. and C. L. Axness (1983), Three-dimensional stochastic analysis of macrodispersion in
1299 aquifers. *Water Resour. Res.*, **19**, 161-180.
1300 Gelhar, L.W., C. Welty and K. R. Rehfeldt (1992), A critical review of data on field-scale dispersion in
1301 aquifers. *Water Resour. Res.*, **28**, 1955-1974.
1302 Gladkikh, M., D. Jacobi, and F. Mendez (2007), Pore geometric modeling for petrophysical interpretation
1303 of downhole formation evaluation data, *Water Resour. Res*., 43(12),
1304 W12s08,DOI:10.1029/2006wr005688.
1305 Gomez-Hernandez, J.J. and S. M. Gorelick (1989), Effective groundwater model parameter values;
1306 influence of spatial variability of hydraulic conductivity, leakance, and recharge. *Water*
1307 *Resour. Res*., **25**, 405-419.
1308 Grote, K., S. Hubbard, and Y. Rubin (2003), Field-scale estimation of volumetric water content using
1309 ground-penetrating radar ground wave techniques*, Water Resour. Res*., **39**(11),
1310 1321,DOI:10.1029/2003wr002045.
1311 Hatch, C. E., A. T. Fisher, J. S. Revenaugh, J. Constantz, and C. Ruehl (2006), Quantifying surface water-
1312 groundwater interactions using time series analysis of streambed thermal records: Method
1313 development, *Water Resour. Res*., **42**(10), W10410,DOI:10.1029/2005wr004787.
1314 Hauck C., M. Bottcher and H. Maurer (2010), A new model for quantifying subsurface ice content based
1315 on geophysical datasets. *The Cryoshpere Discuss,* **4**, 787–821.
1316 Hayley, K., L. R. Bentley and M. Gharibi (2009), Time-lapse electrical resistivity monitoring of salt-
1317 affected soil and groundwater, *Water Resour. Res*., **45**. DOI: 10.1029/2008wr007616.
1318 He, X., J. Koch, T. O. Sonnenborg, F. Jorgensen, C. Schamper, and J. C. Refsgaard (2014), Transition
1319 probability- based stochastic geological modeling using airborne geophysical data and
1320 borehole data, *Water Resour. Res*., **50**(4), 3147 3169, DOI:10.1002/2013wr014593.
1321 Hedberg, S. A., R. J. Knight, A. L. Mackay, and K. P. Whittall (1993), The use of nuclear-magnetic
1322 resonance for studying and detecting hydrocarbon contaminants in porous rocks, *Water*
1323 *Resour. Res.*, **29**(4), 1163-1170,DOI:10.1029/92wr02540.
1324 Herckenrath, D., E. Auken, L. Christiansen, A. A. Behroozmand, and P. Bauer-Gottwein (2012), Coupled
1325 hydrogeophysical inversion using time-lapse magnetic resonance sounding and time-lapse
1326 gravity data for hydraulic aquifer testing: Will it work in practice?, *Water Resour. Res*., **48**,
1327 W01539,DOI:10.1029/2011wr010411.

1328 Hermans, T., A. Vandenbohede, L. Lebbe, R. Martin, A. Kemna, J. Beaujean, F. Nguyen (2012), Imaging
1329 artificial salt water infiltration using electrical resistivity tomography constrained by
1330 geostatistical data, *J. Hydrol*., **438**-**439**, 168-180.
1331 Hinedi, Z. R., Z. J. Kabala, T. H. Skaggs, D. B. Borchardt, R. W. K. Lee, and A. C. Chang (1993), Probing soil
1332 and aquifer material porosity with nuclear-magnetic resonance, *Water Resour. Res*., **29**(12),
1333 3861-3866,DOI:10.1029/93wr02302.
1334 Hinedi, Z. R., A. C. Chang, M. A. Anderson, and D. B. Borchardt (1997), Quantification of microporosity by
1335 nuclear magnetic resonance relaxation of water imbibed in porous media, *Water Resour.*
1336 *Res*., **33**(12), 2697-2704,DOI:10.1029/97wr02408.
1337 Hinnell, A.C., T. P. A. Ferre, J. A. Vrugt, J. A. Huisman, S. Moysey, J. Rings and M. B. Kowalsky, (2010),
1338 Improved extraction of hydrologic information from geophysical data through coupled
1339 hydrogeophysical inversion, *Water Resour. Res*., **46**, W00D40,
1340 DOI:10.1029/2008WR007060.
1341 Hirano, Y., R. Yamamoto, M. Dannoura, K. Aono, T. Igarashi, M. Ishii, K. Yamase, N. Makita and Y.
1342 Kanazawa (2012), Detection frequency of Pinus thunbergii roots by ground-penetrating
1343 radar is related to root biomass, *Plant Soil*, **360**, 363–373, DOI 10.1007/s11104-012-1252-1
1344 Holden, J. (2005), Piping and woody plants in peatlands: Cause or effect?, *Water Resour. Res*., **41**(6),
1345 W06009,DOI:10.1029/2004wr003909.
1346 Hoversten, G. M., F.Cassassuce, E. Gasperikova, G. A. Newman, J. Chen,Y. Rubin, Z. Hou, and D. Vasco
1347 (2006), Direct reservoir parameter estimation using joint inversion of marine seismic AVA
1348 and CSEM data, *Geophysics*, **71**(3), C1–C13.
1349 Hubbard, S.S., Y. Rubin and E. Majer (1997), Ground-penetrating-radar-assisted saturation and
1350 permeability estimation in bimodal systems, *Water Resour. Res*., **33**, 971-990.
1351 Hubbard, S.S., Y. Rubin and E. Majer (1999), Spatial correlation structure estimation using geophysical
1352 and hydrogeological data, *Water Resour. Res*., **35**, 1809-1825.
1353 Hubbard, S.S., J. S. Chen, J. Peterson, E. L. Majer, K. H. Williams, D. J. Swift, B. Mailloux and Y. Rubin
1354 (2001), Hydrogeological characterization of the South Oyster Bacterial Transport Site using
1355 geophysical data, *Water Resour. Res*., **37**, 2431-2456.
1356 Hubbard, S. S., Gangodagamage, C., Dafflon, B., Wainwright, H., Peterson, J. E., Gusmeroli, A., Ulrich, C.,
1357 Wu, Y., Wilson, C., Rowland, J., Tweedie, C., and S.D. Wullschleger (2013), Quantifying and
1358 relating land-surface and subsurface variability in permafrost environments using LiDAR and
1359 surface geophysical datasets, *Hydrogeology*, DOI: 10.1007/s10040-012-0939-y.

1360 Huisman, J.A., C. Sperl, W. Bouten and J.M. Verstraten (2001), Soil water content measurements at
1361 different scales: accuracy of time domain reflectometry and ground-penetrating radar, *J.*
1362 *Hydrol.*, **245**(1-4), 48-58.
1363 Huisman, J.A., J.J.J.C. Snepvangers, W. Bouten and G.B.M. Heuvelink (2002), Mapping spatial variation in
1364 surface soil water content: comparison of ground-penetrating radar and time domain
1365 reflectometry, *J. Hydrol.*, **269**(3-4), 194-207.
1366 Huisman, J.A., S.S. Hubbard, J.D. Redman and P.A. Annan (2003), Measuring soil water content with
1367 ground penetrating radar: a review, *Vadose Zone J.*, **2**(4), 476-491.
1368 Huisman, J.A., J. Rings, J.A. Vrugt, J. Sorg and H. Vereecken (2010), Hydraulic properties of a model dike
1369 from coupled Bayesian and multi-criteria hydrogeophysical inversion, *J. Hydrol.*, **380**, 62-73.
1370 Huth, N.I. and P.L. Poulton (2007), An electromagnetic induction method for monitoring variation in soil
1371 moisture in agroforestry systems. *Aust. J. Soil Res*. **45** (1), 63–72.
1372 Hyndman, D. W., and S. M. Gorelick (1996), Estimating lithologic and transport properties in three
1373 dimensions using seismic and tracer data: The Kesterson aquifer, *Water Resour. Res*., **32**(9),
1374 2659-2670,DOI:10.1029/96wr01269.
1375 Hyndman, D.W., J. M. Harris and S. M. Gorelick (1994) Coupled seismic and tracer test inversion for
1376 aquifer property characterization. *Water Resour. Res*., **30**, 1965-1977.
1377 Ikard, S. J., A. Revil, A. Jardani, W. F. Woodruff, M. Parekh, and M. Mooney (2012), Saline pulse test
1378 monitoring with the self-potential method to non intrusively determine the velocity of the
1379 pore water in leaking areas of earth dams and embankments, *Water Resour. Res*., **48**,
1380 W04201, DOI:10.1029/2010WR010247.
1381 Ioannidis, M. A., I. Chatzis, C. Lemaire, and R. Perunarkilli (2006), Unsaturated hydraulic conductivity
1382 from nuclear magnetic resonance measurements, *Water Resour. Res*., **42**(7),
1383 W07201DOI:10.1029/2006wr004955.
1384 Irving J.D. and K. Singha (2010), Stochastic inversion of tracer test and electrical geophysical data to
1385 estimate hydraulic conductivities, *Water Resour. Res*., **46**, W11514,
1386 DOI:11510.11029/12009WR008340.
1387 Irving, J., R. Knight, and K. Holliger (2009), Estimation of the lateral correlation structure of subsurface
1388 water content from surface-based ground-penetrating radar reflection images, *Water*
1389 *Resour. Res*., **45**, W12404,DOI:10.1029/2008wr007471.

Jackson R.B., E.G. Jobbagy R. Avissar, S.B. Roy, D.J. Barrett, C.W. Cook, K.A. Farley, D.C. le Maitre, B.A. McCarl and B.C. Murray (2005), Trading water for carbon with biological sequestration. *Science*, **310**, 1944–1947

JafarGandomi, A., and A. Binley (2013), A Bayesian trans-dimensional approach for the fusion of multiple geophysical datasets, *Journal of Applied Geophysics*, **96**, 38-54,DOI:10.1016/j.jappgeo.2013.06.004.

Jardani, A., A. Revil, and J.P. Dupont (2013), Stochastic joint inversion of hydrogeophysical data for salt tracer test monitoring and hydraulic conductivity imaging, *Advances in Water Resources*, **52**, 62-77, DOI: 10.1016/j.advwatres.2012.08.005.

Jayawickreme D.H., R.L. Van Dam and D.W. Hyndman (2008), Subsurface imaging of vegetation, climate, and root-zone moisture interactions. *Geophysical Research Letters,* **35**, L18404.

Jayawickreme D.H., R.L. Van Dam and D.W. Hyndman (2010), Hydrological consequences of land-cover change: Quantifying the influence of plants on soil moisture with time-lapse electrical resistivity. *Geophysics*, **75**, WA43-WA50.

Jayawickreme D.H., E.G. Jobbagy and R.B. Jackson (2014), Geophysical subsurface imaging for ecological applications. *New Phytologist,* **201**, 1170–1175 DOI: 10.1111/nph.12619

Johnson, T.J., Slater, L., Day-Lewis, F.D., Ntarlagiannis, D. and Elwaseif, M. (2012), Monitoring groundwater/surface-water interaction using time-series and time-frequency analysis of transient three-dimensional electrical resistivity changes, *Water Resour. Res.*, **48**(7), W07506, DOI: 10.1029/2012WR011893

Keery, J., A. Binley, N. Crook and J. W. N. Smith (2007), Temporal and spatial variability of groundwater-surface water fluxes: Development and application of an analytical method using temperature time series, *Journal of Hydrology*, **336**, 1-16. DOI: 10.1016/j.jhydrol.2006.12.003.

Keller, G. V., and F. C. Frischknecht (1966), *Electrical Methods of Geophysical Prospecting, Int. Ser. Monogr. Electromagn. Waves*, vol. 10, Pergamon, Oxford, N. Y.

Kemna, A., J. Vanderborght, B. Kulessa, and H. Vereecken (2002), Imaging and characterisation of subsurface solute transport using electrical resistivity tomography (ERT) and equivalent transport models*, J. Hydrol.*, **267**(3–4), 125–146, doi:10.1016/S0022-1694(02)00145-2.

Killey, R. W. D., and G. L. Moltyaner (1988), Twin Lake tracer tests – Setting, methodology, and hydraulic conductivity distribution, *Water Resour. Res.*, 24(10), 1585-1612,doi:10.1029/WR024i010p01585.

1422 Kim, J. H., M.J. Yi, S.G. Park, and J.G. Kim (2009), 4-D inversion of DC resistivity monitoring data acquired
1423 over a dynamically changing earth model: *J. Appl. Geophys.*, **68**, 4, 522-532.
1424 Karaoulis, M. C., J.H. Kim, and P.I. Tsourlos (2011), 4D active time constrained resistivity inversion, *J.*
1425 *Appl. Geophys.,* **73**, 1, 25-34.
1426 Kirkegaard, C., T. O. Sonnenborg, E. Auken, and F. Jorgensen (2011), Salinity Distribution in
1427 Heterogeneous Coastal Aquifers Mapped by Airborne Electromagnetics, *Vadose Zone*
1428 *Journal*, **10**(1), 125-135,DOI:10.2136/vzj2010.0038.
1429 Koestel, J., A. Kemna, M. Javaux, A. Binley and H. Vereecken (2008), Quantitative imaging of solute
1430 transport in an unsaturated and undisturbed soil monolith with 3-D ERT and TDR, *Water*
1431 *Resour. Res*., **44**, W12411, DOI:12410.11029/12007WR006755.
1432 Kowalsky, M., S. Finsterle, J. Peterson, S. Hubbard, Y. Rubin, E. Majer, A. Ward and G. Gee (2005),
1433 Estimation of field-scale soil hydraulic and dielectric parameters through joint inversion of
1434 GPR and hydrological data, *Water Resour. Res.*, **41**(11), DOI: 10.1029/2005WR004237.
1435 Laloy, E., N. Linde, and J. A. Vrugt (2012), Mass conservative three-dimensional water tracer distribution
1436 from Markov chain Monte Carlo inversion of time-lapse ground-penetrating radar data,
1437 *Water Resour. Res.*, **48**, doi:W0751010.1029/2011wr011238.Lambot, S., L. Weihermuller, J.
1438 A. Huisman, H. Vereecken, M. Vanclooster, and E. C. Slob (2006), Analysis of air-launched
1439 ground-penetrating radar techniques to measure the soil surface water content, *Water*
1440 *Resour. Res.*, **42**(11), W11403,DOI:10.1029/2006wr005097.
1441 LeBlanc, D.R., S. P. Garabedian, K. M. Hess, L. W. Gelhar, R. D. Quadri, K. G. Stollenwerk and W. W. Wood
1442 (1991), Large-scale natural gradient tracer test in sand and gravel, Cape Cod,
1443 Massachusetts: 1. Experimental design and observed tracer movement. *Water Resour. Res.*,
1444 **27**, 895-910.
1445 LaBrecque, D. and X. Yang (2001), Difference Inversion of ERT Data: Fast Inversion Method for 3D In Situ
1446 Monitoring, *Journal of Environmental and Engineering Geophysics*, 6(2), 83-89.
1447 Lelièvre, P.G. and C.G. Farquharson (2014), Gradient and smoothness regularization operators for
1448 geophysical inversion on unstructured meshes, *Geophys. J. Int.*, **195**, 330-341, DOI:
1449 10.1093/gji/ggt255.
1450 Lendvay, J. M., W. A. Sauck, M. L. McCormick, M. J. Barcelona, D. H. Kampbell, J. T. Wilson, and P.
1451 Adriaens (1998), Geophysical characterization, redox zonation, and contaminant
1452 distribution at a groundwater surface water interface, *Water Resour. Res.*, **34**(12), 3545-
1453 3559,doi:10.1029/98wr01736.

1454 Li, C., P. Tercier, and R. Knight (2001), Effect of sorbed oil on the dielectric properties of sand and clay,
1455 *Water Resour. Res.*, **37**(6), 1783-1793,DOI:10.1029/2001wr900006.
1456 Li, L. and D.W. Oldenburg (2003), Fast inversion of large-scale magnetic data using wavelet transforms
1457 and a logarithmic barrier method, *Geophys. J. Int.*, **152**, 251–265.
1458 Li, Z.,Y. Liu, Y. Zheng and R. Xu (2015), Zeta potential at the root surfaces of rice characterized by
1459 streaming potential measurements, *Plant Soil*, **386**, 237–250, DOI 10.1007/s11104-014-
1460 2259-6
1461 Linde, N., A. Binley, A. Tryggvason, L. B. Pedersen and A. Revil (2006), Improved hydrogeophysical
1462 characterization using joint inversion of cross-hole electrical resistance and ground-
1463 penetrating radar traveltime data, *Water Resour. Res.*, **42**, W12404,
1464 DOI:12410.11029/12006WR005131.
1465 Looms, M.C., A. Binley, K. H. Jensen, L. Nielsen and T. M. Hansen (2008), Identifying unsaturated
1466 hydraulic parameters using an integrated data fusion approach on cross-borehole
1467 geophysical data, *Vadose Zone Journal*, **7**, 238-248.
1468 Lunt, I., S.S. Hubbard, Y. Rubin (2005), Soil moisture estimation using ground-penetrating radar
1469 reflection data, *Journal of Hydrology*, **307**, 254-269.
1470 Macleod, C.J.A, M. W. Humphreys, W. R. Whalley, L. Turner, A.Binley, C. W. Watts, L. Skøt, A. Joynes, S.
1471 Hawkins, I. P. King, S. O'Donovan, P. M. Haygarth (2013), A novel grass hybrid to reduce
1472 flood generation in temperate regions, *Nature Scientific Reports*, **3**, 1683, DOI:
1473 10.1038/srep01683.
1474 Mateeva, A., J. Lopez, H. Potters, J. Mestayer, B. Cox, D. Kiyashchenko, P. Wills, S. Grandi, K. Hornman, B.
1475 Kuvshinov, W. Berlang, Z. Yang, and R. Detomo (2014), Distributed acoustic sensing for
1476 reservoir monitoring with vertical seismic profiling, *Geophysical Prospecting*, **62**(4), 679-
1477 692,DOI:10.1111/1365-2478.12116.
1478 McKenna S. and E. P. Poeter (1995), Field example of data fusion in site characterization, *Water Resour.*
1479 *Res.*, **31**, 3229-3240.
1480 Merz, B., and E. J. Plate (1997), An analysis of the effects of spatial variability of soil and soil moisture on
1481 runoff, *Water Resour. Res.*, **33**(12), 2909-2922,DOI:10.1029/97wr02204.
1482 Meyerhoff, S. B., R. M. Maxwell, A. Revil, J. B. Martin, M. Karaoulis, and W. D. Graham (2014),
1483 Characterization of groundwater and surface water mixing in a semiconfined karst aquifer
1484 using time- lapse electrical resistivity tomography, *Water Resour. Res.*, **50**(3), 2566-
1485 2585,DOI:10.1002/2013wr013991.

Michot, D., Y. Benderitter, A. Dorigny, B. Nicoullaud, D. King and A. Tabbagh (2003), Spatial and temporal monitoring of soil water content with an irrigated corn crop cover using surface electrical resistivity tomography. *Water Resour. Res.,* **39**, 1138. DOI:10.1029/2002WR001518.

Miled, M. B. H. and E.L. Miller (2007), A projection-based level-set approach to enhance conductivity anomaly reconstruction in electrical resistance tomography, *Inverse Problems*, **23**(6), 2375-2400, doi:10.1088/0266-5611/23/6/007.

Minsley, B. J., J. Sogade, and F. D. Morgan (2007), Three-dimensional self-potential inversion for subsurface DNAPL contaminant detection at the Savannah River Site, South Carolina, *Water Resour. Res.*, **43**(4), W04429, DOI:10.1029/2005wr003996.

Minsley, B. J., J.D. Abraham, B.D. Smith, J.C. Cannia, C.I. Voss, M.T.Jorgenson, M.A. Walvoord, B.K. Wylie, L.Anderson, L.Bl Ball, M.Deszcz-Pan, T.P. Wellman and T.A. Ager (2012*),* Airborne electromagnetic imaging of discontinuous permafrost*, Geophys. Res. Lett.,* **39***, L02503,* DOI:10.1029/2011GL050079*.*

Mohnke, O., and B. Hughes (2014), Jointly deriving NMR surface relaxivity and pore size distributions by NMR relaxation experiments on partially desaturated rocks, *Water Resour. Res*., **50**(6), 5309-5321,DOI:10.1002/2014wr015282.

Moltyaner, G. L., and C. A. Wills (1991), Local-scale and plume-scale dispersion in the Twin Lake 40-m and 260-m natural gradient tracer tests, *Water Resour. Res.*, **27**(8), 2007-2026,doi:10.1029/91wr01147.

Monteiro Santos, F.A., A.R. Andrade Afonso and A. Dupis (2007), 2D joint inversion of dc and scalar audio-magnetotelluric data in evaluation of low enthalpy geothermal fields, *Journal of Geophysics and Engineering*, **4**, 53-62.

Moysey, S. and R. Knight (2004), Modeling the field-scale relationship between dielectric constant and water content in heterogeneous systems, *Water Resour. Res.*, **40**, W03510, DOI:03510.01029/02003WR002589.

Mualem, Y., and S. P. Friedman (1991), Theoretical prediction of electrical-conductivity in saturated and unsaturated soil, *Water Resour. Res.*, **27**(10), 2771-2777,DOI:10.1029/91wr01095.

Neuman, S.P. (1990), Universal scaling of hydraulic conductivities and dispersivities in geologic media. *Water Resour. Res*., **26**, 1749-1758.

Oware, E. K., S. M. J. Moysey, and T. Khan, 2013, Physically based regularization of hydrogeophysical inverse problems for improved imaging of process-driven systems, *Water Resour. Res*., **49**, 6238–6247, DOI:10.1002/wrcr.20462.

1518 Paine, J. G. (2003), Determining salinization extent, identifying salinity sources, and estimating chloride
1519 mass using surface, borehole, and airborne electromagnetic induction methods, *Water*
1520 *Resour. Res*., **39**(3), 1059,DOI: 10.1029/2001wr000710.
1521 Panissod, C., M. Dabas, A. Hesse, A. Jolivet, J. Tabbagh and A. Tabbagh (1998), Recent developments in
1522 shallow-depth electrical and electrostatic prospecting using mobile arrays, *Geophysics*,
1523 **63**(5), 1542–1550
1524 Parkin, G., D. Redman, P. von Bertoldi, and Z. Zhang (2000), Measurement of soil water content below a
1525 wastewater trench using ground-penetrating radar, *Water Resour. Res.*, **36**(8), 2147-
1526 2154,DOI:10.1029/2000wr900129.
1527 Parra, J. O., C. L. Hackert, and M. W. Bennett (2006), Permeability and porosity images based on P-wave
1528 surface seismic data: Application to a south Florida aquifer, *Water Resour. Res.,* **42**(2),
1529 W02415,DOI:10.1029/2005wr004114.
1530 Parsekian, A. D., L. Slater, and D. Gimenez (2012), Application of ground-penetrating radar to measure
1531 near-saturation soil water content in peat soils, *Water Resour. Res.*, **48**, W02533, DOI:
1532 10.1029/2011wr011303.
1533 Pickens, J. F., and G. E. Grisak (1981), Scale-dependent dispersion in a stratified granular aquifer, *Water*
1534 *Resour. Res.*, **17**(4), 1191-1211, DOI:10.1029/WR017i004p01191.
1535 Pidlisecky, A., K. Singha, and F.D. Day-Lewis (2011), A distribution-based parameterization for improved
1536 tomographic imaging of solute plumes, *Geophys. J. Int.*, **187**(1), doi: 10.1111/j.1365-
1537 246X.2011.05131.x.
1538 Pollock, D.W. and O. A. Cirpka (2012), Fully coupled hydrogeophysical inversion of a laboratory salt
1539 tracer experiment monitored by electrical resistivity tomography, *Water Resour. Res*., **48**,
1540 W01505, DOI:01510.01029/02011WR010779.
1541 Purvance, D. T. and R. Andricevic (2000), On the electrical-hydraulic conductivity correlation in aquifers,
1542 *Water Resour. Res.*, **36**, 2905-2913.
1543 Ramirez, A., W. Daily, D. Labrecque, E. Owen and D. Chesnut (1993), Monitoring an underground steam
1544 injection process using electrical resistance tomography. *Water Resour. Res*., **29**, 73-87.
1545 Rawlins, B.G., B. P. Marchant, D. Smyth, C. Scheib, R. M. Lark and C. Jordan (2009), Airborne radiometric
1546 survey data and a DTM as covariates for regional scale mapping of soil organic carbon
1547 across Northern Ireland, *European Journal of Soil Science*, **60**(1), 44-54, DOI:
1548 10.1111/j.1365-2389.2008.01092.x.

1549 Rea, J. and R. Knight (1998), Geostatistical analysis of ground-penetrating radar data: A means of
1550 describing spatial variation in the subsurface, *Water Resour. Res.*, **34**, 329-339.
1551 Regberg, A., K. Singha, M. Tien, F. Picardal, Q. Zheng, J. Schieber, E. Roden and S. L. Brantley (2011),
1552 Electrical conductivity as an indicator of iron reduction rates in abiotic and biotic systems,
1553 *Water Resour. Res.*, **47**, W04509, DOI:04510.01029/02010WR009551.
1554 Rehfeldt, K.R., J. M. Boggs and L. W. Gelhar (1992), Field study of dispersion in a heterogeneous aquifer;
1555 3, Geostatistical analysis of hydraulic conductivity. *Water Resour. Res.*, **28**, 3309-3324.
1556 Revil, A. (2012), Spectral induced polarization of shaly sands: Influence of the electrical double layer,
1557 *Water Resour. Res.*, **48**, W02517, DOI:10.1029/2011WR011260.
1558 Revil, A. (2013), Effective conductivity and permittivity of unsaturated porous materials in the frequency
1559 range 1 mHz–1GHz, *Water Resour. Res.*, **49**, 306-327, DOI:10.1029/2012WR012700.
1560 Revil, A., and L. M. Cathles (1999), Permeability of shaly sands, *Water Resour. Res.*, **35**(3), 651-
1561 662,DOI:10.1029/98wr02700.
1562 Revil A. and H. Mahardika (2013), Coupled hydromechanical and electromagnetic disturbances in
1563 unsaturated clayey materials, *Water Resour. Res.*, **49**(2), 744-766, DOI:10.1002/wrcr.2009.
1564 Revil, A., V. Naudet, J. Nouzaret, and M. Pessel (2003), Principles of electrography applied to self-
1565 potential electrokinetic sources and hydrogeological applications, *Water Resour. Res.*,
1566 39(5), 1114, DOI: 10.1029/2001WR000916.
1567 Revil A., C.A. Mendonça, E. Atekwana, B. Kulessa, S.S. Hubbard, and K. Bolhen (2010), Understanding
1568 biogeobatteries: where geophysics meets microbiology, *Journal of Geophysical Research*,
1569 **115**, G00G02, DOI:10.1029/2009JG001065.
1570 Revil, A., K. Koch, and K. Holliger (2012a), Is it the grain size or the characteristic pore size that controls
1571 the induced polarization relaxation time of clean sands and sandstones? *Water Resour.*
1572 *Res.*, **48**, W05602, DOI:10.1029/2011WR011561.
1573 Revil, A., E. Atekwana, C. Zhang, A. Jardani, and S. Smith (2012b), A new model for the spectral induced
1574 polarization signature of bacterial growth in porous media, *Water Resour. Res.*, **48**,
1575 W09545, DOI:10.1029/2012WR011965.
1576 Revil A., G. Barnier, M. Karaoulis, and P. Sava (2014a), Seismoelectric coupling in unsaturated porous
1577 media: Theory, petrophysics, and saturation front localization using an electroacoustic
1578 approach, *Geophysical Journal International*, **196**(2), 867-884, DOI: 10.1093/gji/ggt440.

1579 Revil, A., P. Kessouri, and C. Torres-Verdín (2014b), Electrical conductivity, induced polarization, and
1580 permeability of the Fontainebleau sandstone, *Geophysics*, **79**(5), D301–D318, doi:
1581 10.1190/GEO2014-0036.1
1582 Roberts J.J. and W. N. Lin (1997), Electrical properties of partially saturated Topopah Spring tuff: Water
1583 distribution as a function of saturation, *Water Resour. Res.*, **33**, 577-587.
1584 Robinson, D., S. Jones, J. Wraith, J., D. Or, and S. Friedman (2003), A review of advances in dielectric
1585 and electrical conductivity measurement in soils using time domain reflectometry, *Vadose*
1586 *Zone J.*, **2**, 444–475.
1587 Robinson, D.A., Schaap M.G., Or D. and Jones S.B. (2005), On the effective measurement frequency of
1588 TDR in dispersive and non-conductive dielectric materials. *Water Res Res.*, **41**, W02007,
1589 DOI:10.1029/2004WR003816.
1590 Robinson, D. A., A. Binley, N. Crook, F. D. Day-Lewis, T. P. A. Ferre, V. J. S. Grauch, R. Knight, M. Knoll, V.
1591 Lakshmi, R. Miller, J. Nyquist, L. Pellerin, K. Singha, and L. Slater (2008a), Advancing process-
1592 based watershed hydrological research using near-surface geophysics: A vision for, and
1593 review of, electrical and magnetic geophysical methods, *Hydrol. Processes*, **22**, 3604– 3635,
1594 DOI:10.1002/hyp.6963.
1595 Robinson, D.A., Abdu H., Jones S.B., Seyfried M. Lebron I., and Knight R. (2008b), Eco-Geophysical
1596 Imaging of Watershed-Scale Soil Patterns Links with Plant Community Spatial Patterns.
1597 *Vadose Zone Journal*, **7**(4), 1132-1138.
1598 Robinson, D. A., I. Lebron, B. Kocar, K. Phan, M. Sampson, N. Crook, and S. Fendorf (2009), Time-lapse
1599 geophysical imaging of soil moisture dynamics in tropical deltaic soils: An aid to interpreting
1600 hydrological and geochemical processes, *Water Resour. Res.*, **45**, W00d32,
1601 DOI:10.1029/2008wr006984.
1602 Robinson, D. A., I. Lebron and J.I. Querejeta (2010), Determining Soil-Tree-Grass Relationships in a
1603 California Oak Savanna Using Eco-Geophysics. *Vadose Zone Journal*, **9**(1), 1-8.
1604 Robinson D.A. H. Abdu, I. Lebron, S.B. Jones (2012), Imaging of hill-slope soil moisture wetting patterns
1605 in a semi-arid oak savanna catchment using time-lapse electromagnetic induction. *Journal*
1606 *of Hydrology*, DOI:10.1016/j.jhydrol.2011.11.034
1607 Rodrigues, F.A., R.G. V. Bramley and D.L. Gobbett (2015), Proximal soil sensing for precision agriculture:
1608 simultaneous use of electromagnetic induction and gamma radiometrics in contrasting
1609 soils, *Geoderma*, 243-244, 183-195, doi:10.1016/j.geoderma.2015.01.004
1610 Rubin, Y., and S. S. Hubbard (2005), *Hydrogeophysics*, 523 pp., Springer, New York.

1611 Rubin, Y., G. Mavko and J. Harris (1992), Mapping permeability in heterogeneous aquifers using
1612 hydrologic and seismic data. *Water Resour. Res.*, **28**, 1809-1816.
1613 Rucker, D. F., G. E. Noonan, and W. J. Greenwood (2011), Electrical resistivity in support of geological
1614 mapping along the Panama Canal, *Engineering Geology*, **117**, 1-2, 121–133.
1615 Saarenketo, T. (1998), Electrical properties of water in clay and silty soils, *J. Appl. Geophys.*, **40**(1-3), 73–
1616 88.
1617 Sassen, D. S., S. S. Hubbard, S. A. Bea, J. Chen, N. Spycher, and M. E. Denham (2012), Reactive facies: An
1618 approach for parameterizing field-scale reactive transport models using geophysical
1619 methods, *Water Resour. Res.*, **48**, W10526,DOI:10.1029/2011wr011047.
1620 Sava P., A. Revil, and M. Karaoulis (2014), Cross-well electrical resistivity imaging using seismoelectric
1621 focusing and image-guided inversion, *Geophysical Journal International*, **198**, 880–894, DOI:
1622 10.1093/gji/ggu166.
1623 Scheibe, T.D. and Y.J. Chien (2003), An evaluation of conditioning data for solute transport prediction,
1624 *Ground Water*, **41**(2), 128-41.
1625 Scheibe T.D., Y. Fang, C.J. Murray, E.E. Roden, J. Chen, Y.J. Chien, S.C. Brooks, and S.S. Hubbard (2006),
1626 Transport and biogeochemical reaction of metals in a physically and chemically
1627 heterogeneous aquifer, *Geosphere*, **2**(4),220-235.
1628 Scholer, M., J. Irving, A. Binley and K. Holliger (2011), Estimating vadose zone hydraulic properties using
1629 ground penetrating radar: The impact of prior information, *Water Resour. Res.,* **47**,
1630 W10512.
1631 Schulze-Makuch, D., D.A. Carlson, D.S. Cherkauer and P. Malik (1999), Scale Dependency of Hydraulic
1632 Conductivity in Heterogeneous Media, *Ground Water,* **37**(6), 904-919, DOI: 10.1111/j.1745-
1633 6584.1999.tb01190.x.
1634 Selker, J. S., L. Thevenaz, H. Huwald, A. Mallet, W. Luxemburg, N. v. de Giesen, M. Stejskal, J. Zeman, M.
1635 Westhoff, and M. B. Parlange (2006), Distributed fiber-optic temperature sensing for
1636 hydrologic systems, *Water Resour. Res.*, **42**(12), W12202,DOI:10.1029/2006wr005326.
1637 Shanahan, P., A. Binley, R. Whalley and C. Watts, 2015, The use of electromagnetic induction (EMI) to
1638 monitor changes in soil moisture profiles beneath different wheat cultivars, *Soil Sci. Soc.*
1639 *Am. J.*, **79**, 459–466, DOI: 10.2136/sssaj2014.09.0360.
1640 Shefer, I., N. Schwartz, and A. Furman (2013), The effect of free-phase NAPL on the spectral induced
1641 polarization signature of variably saturated soil, *Water Resour. Res.*, **49**(10),6229-
1642 6237,DOI:10.1002/wrcr.20502.

1643 Sherlock, M. D., and J. J. McDonnell (2003), A new tool for hillslope hydrologists: Spatially distributed
1644 groundwater level and soil water content measured using electromagnetic induction,
1645 *Hydrol. Processes*, **17**, 1965– 1977, DOI:10.1002/hyp.1221.
1646 Siemon, B., E. Auken, and A. V. Christiansen (2009), Laterally constrained inversion of helicopter-borne
1647 frequency-domain electromagnetic data, *Journal of Applied Geophysics*, **67**(3), 259-
1648 268,DOI:10.1016/j.jappgeo.2007.11.003.
1649 Singha K. and S. M. Gorelick (2005), Saline tracer visualized with three-dimensional electrical resistivity
1650 tomography: Field-scale spatial moment analysis, *Water Resour. Res.*, **41**, W05023,
1651 DOI:05010.01029/02004WR003460.
1652 Singha, K. , F.D. Day-Lewis and J.W. Lane (2007), Geoelectrical evidence of bicontinuum transport in
1653 groundwater, *Geophysical Research Letters*, **34**(12), L12401, doi:10.1029/2007GL030019.
1654 Slater, L. and D.P. Lesmes (2002), Electrical-hydraulic relationships observed for unconsolidated
1655 sediments, *Water Resour. Res.*, **38**, 1-13.
1656 Slater, L., X. Comas, D. Ntarlagiannis and M. R. Moulik (2007), Resistivity-based monitoring of biogenic
1657 gases in peat soils, *Water Resour. Res.*, **43**, W10430, DOI:10410.11029/12007WR006090.
1658 Slater, L. D., F. D. Day-Lewis, D. Ntarlagiannis, M. O'Brien, *and* N. Yee (2009*),* Geoelectrical measurement
1659 and modeling of biogeochemical breakthrough behavior during microbial activity*, Geophys.*
1660 *Res. Lett.,* **36***, L14402,* DOI: 10.1029/2009GL038695.
1661 Slater, L.D., D. Ntarlagiannis, F. D. Day-Lewis, K. Mwakanyamale, R. J. Versteeg, A. Ward, C. Strickland, C.
1662 D. Johnson and J. W. Lane, Jr. (2010), Use of electrical imaging and distributed temperature
1663 sensing methods to characterize surface water-groundwater exchange regulating uranium
1664 transport at the Hanford 300 Area, Washington, *Water Resour. Res.*, **46**, W10533,
1665 DOI:10510.11029/12010WR009110.
1666 Slater, L., W. Barrash, J. Montrey, and A. Binley (2014), Electrical-hydraulic relationships observed for
1667 unconsolidated sediments in the presence of a cobble framework, *Water Resour. Res.*,
1668 **50**(7), 5721-5742,DOI:10.1002/2013wr014631.
1669 Stingaciu, L. R., L. Weihermueller, S. Haber-Pohlmeier, S. Stapf, H. Vereecken, and A. Pohlmeier (2010),
1670 Determination of pore size distribution and hydraulic properties using nuclear magnetic
1671 resonance relaxometry: A comparative study of laboratory methods, *Water Resour. Res.*,
1672 **46**, W11510,DOI:10.1029/2009wr008686.

1673 Strobach, E., B. D. Harris, J. C. Dupuis, and A. W. Kepic (2014), Time-lapse borehole radar for monitoring
1674 rainfall infiltration through podosol horizons in a sandy vadose zone, *Water Resour. Res.*,
1675 **50**(3), 2140-2163,DOI:10.1002/2013wr014331.
1676 Sudduth, K. A., S. T. Drummond, and N. R. Kitchen (2001), Accuracy issues in electromagnetic induction
1677 sensing of soil electrical conductivity for precision agriculture, *Computers and Electronics in*
1678 *Agriculture*, **31**(3), 239-264,DOI:10.1016/s0168-1699(00)00185-x.
1679 Swanson, R., K. Singha, F. D. Day-Lewis, A. Binley, K. Keating and R. Haggerty (2012), Direct geoelectrical
1680 evidence of mass transfer at the laboratory scale, *Water Resour. Res.*, **48**,
1681 DOI:10.1029/2012WR012431.
1682 Tarantola, A. (2005), *Inverse Problem Theory. Methods for model parameter estimation*: Society of
1683 Industrial and Applied Mathematics
1684 Thomsen, R., V. H. Søndergaard, and K. I. Sørensen (2004), Hydrogeological mapping as a basis for
1685 establishing site-specific groundwater protection zones in Denmark, *Hydrogeology Journal*,
1686 **12**(5), 550-562.
1687 Tikhonov, A. N., and V. A. Arsenin (1977), *Solution of Ill-Posed Problems* John Wiley, New York, 258 pp.
1688 Topp, G.C., J. L. Davis and A. P. Annan (1980), Electromagnetic determination of soil water content:
1689 measurements in coaxial transmission lines. *Water Resour. Res.*, **16**, 574-582.
1690 Tsoflias, G. P., T. Halihan, and J. M. Sharp (2001), Monitoring pumping test response in a fractured
1691 aquifer using ground-penetrating radar, *Water Resour. Res.*, **37**(5), 1221-
1692 1229,DOI:10.1029/2000wr900297.
1693 Tyler, S.W., J. S. Selker, M. B. Hausner, C. E. Hatch, T. Torgersen, C. E. Thodal and S. G. Schladow (2009),
1694 Environmental temperature sensing using Raman spectra DTS fiber-optic methods, *Water*
1695 *Resour. Res.*, **45**, DOI: 10.1029/2008wr007052.
1696 Urish, D.W. (1981), Electrical resistivity-hydraulic conductivity relationships in glacial outwash aquifers.
1697 *Water Resour. Res.*, **17**, 1401-1407.
1698 Van Dam, R. L., B. P. Eustice, D. W. Hyndman, W. W. Wood, and C. T. Simmons (2014), Electrical imaging
1699 and fluid modeling of convective fingering in a shallow water-table aquifer, *Water Resour.*
1700 *Res.*, **50**(2), 954-968,DOI:10.1002/2013wr013673.
1701 van Dijk, A. (2004), Ecohydrology: It's all in the game. *Hydrol. Process.,* **18**,3683–3686.
1702 Vanderborght, J., A. Kemna, H. Hardelauf and H. Vereecken (2005), Potential of electrical resistivity
1703 tomography to infer aquifer transport characteristics from tracer studies: A synthetic case
1704 study, *Water Resour. Res.*, **41**, W06013, DOI:06010.01029/02004WR003774.

1705 Vaudelet P., A. Revil, M. Schmutz, M. Franceschi, and P. Bégassat (2011), Induced polarization signature
1706 of the presence of copper in saturated sands, *Water Resour. Res.*, **47**, W02526,
1707 DOI:10.1029/2010WR009310.
1708 Vereecken, H., A. Binley, G. Cassiani, A. Revil and K. Titov (2006), *Applied Hydrogeophysics*, Springer,
1709 383pp.
1710 Vilhelmsen, T. N., A. A. Behroozmand, S. Christensen, and T. H. Nielsen (2014), Joint inversion of aquifer
1711 test, MRS, and TEM data, Water Resour. Res., **50**(5), 3956-
1712 3975,DOI:10.1002/2013wr014679.
1713 von Hebel, C., S. Rudolph, A. Mester, J. A. Huisman, P. Kumbhar, H. Vereecken, and J. van der Kruk
1714 (2014), Three-dimensional imaging of subsurface structural patterns using quantitative
1715 large-scale multiconfiguration electromagnetic induction data, *Water Resour. Res.*, **50**(3),
1716 2732-2748,DOI:10.1002/2013wr014864.
1717 Wainwright, H. M., J. Chen, D. S. Sassen, and S. S. Hubbard (2014), Bayesian hierarchical approach and
1718 geophysical data sets for estimation of reactive facies over plume scales, *Water Resour.*
1719 *Res*., **50**(6), 4564-4584,DOI:10.1002/2013wr013842.
1720 Wallin, E.L., T. C. Johnson, W. J. Greenwood and J. M. Zachara (2013), Imaging high stage river-water
1721 intrusion into a contaminated aquifer along a major river corridor using 2-D time-lapse
1722 surface electrical resistivity tomography, *Water Resour. Res.*, **49**, 1693-1708. DOI:
1723 10.1002/Wrcr.20119.
1724 Ward, A., M. Fitzgerald, M. N. Gooseff, T. J. Voltz, A. M. Binley and K. Singha (2012), Hydrologic and
1725 geomorphic controls on hyporheic exchange during base flow recession in a headwater
1726 mountain stream, *Water Resour. Res.*, **48**, W04513, DOI:04510.01029/02011WR011461.
1727 West, L. J., K. Handley, Y. Huang, and M. Pokar (2003), Radar frequency dielectric dispersion in
1728 sandstone: Implications for determination of moisture and clay content, *Water Resour.*
1729 *Res*., **39**(2), 1026,DOI: 10.1029/2001wr000923.
1730 Western, A. W., R. B. Grayson, and G. Bloschl (2002), Scaling of soil moisture: A hydrologic perspective,
1731 *Annu. Rev. Earth Planet. Sci.*, **30**, 149–180, DOI:10.1146/annurev.earth.30.091201.140434.
1732 Williams, K.H., D. Ntarlagiannis, L.D. Slater, A. Dohnalkova, S.S. Hubbard, J.F. Banfield (2005),
1733 Geophysical imaging of stimulated biomineralization, *Environmental Science and*
1734 *Technology,* **39**(19), DOI 10.1021/es0504035
1735 Williams, K.H., A. Kemna, M.J. Wilkins, J. Drfuhan, E. Arntzen, A.L. N'Guessan, P.E. Long, S.S. Hubbard
1736 and J.F. Banfield (2009), Geophysical monitoring of coupled microbial and geochemical

processes during stimulated bioremediation, *Environmental Science and Technology*, **43**(17), 10.1021/es900855j

Woodbury, A. D., and E. A. Sudicky (1991), The geostatistical characteristics of the Borden Aquifer, *Water Resour. Res.*, **27**(4), 533-546,DOI:10.1029/90wr02545.

Worthington, P. F. (1977), Influence of matrix conduction upon hydrogeophysical relationships in arenaceous aquifers, *Water Resour. Res.*, **13**(1), 87-92,DOI:10.1029/WR013i001p00087.

Yeh, P. J.-F., S. C. Swenson, J. S. Famiglietti and M. Rodell (2006), Remote sensing of groundwater storage changes in Illinois using the Gravity Recovery and Climate Experiment (GRACE), *Water Resour. Res.*, **42**(16), W12203, DOI: 10.1029/2006WR005374

Yeh, T.C.J., S. Liu, R. J. Glass, K. Baker, J. R. Brainard, D. Alumbaugh and D. LaBrecque (2002), A geostatistically based inverse model for electrical resistivity surveys and its applications to vadose zone hydrology, *Water Resour. Res.*, **38**, 14-11:14-13.

Zhou, Q.Y., J. Shimada and A. Sato (2001), Three-dimensional spatial and temporal monitoring of soil water content using electrical resistivity tomography, *Water Resour. Res.,* **37**, 273-285.

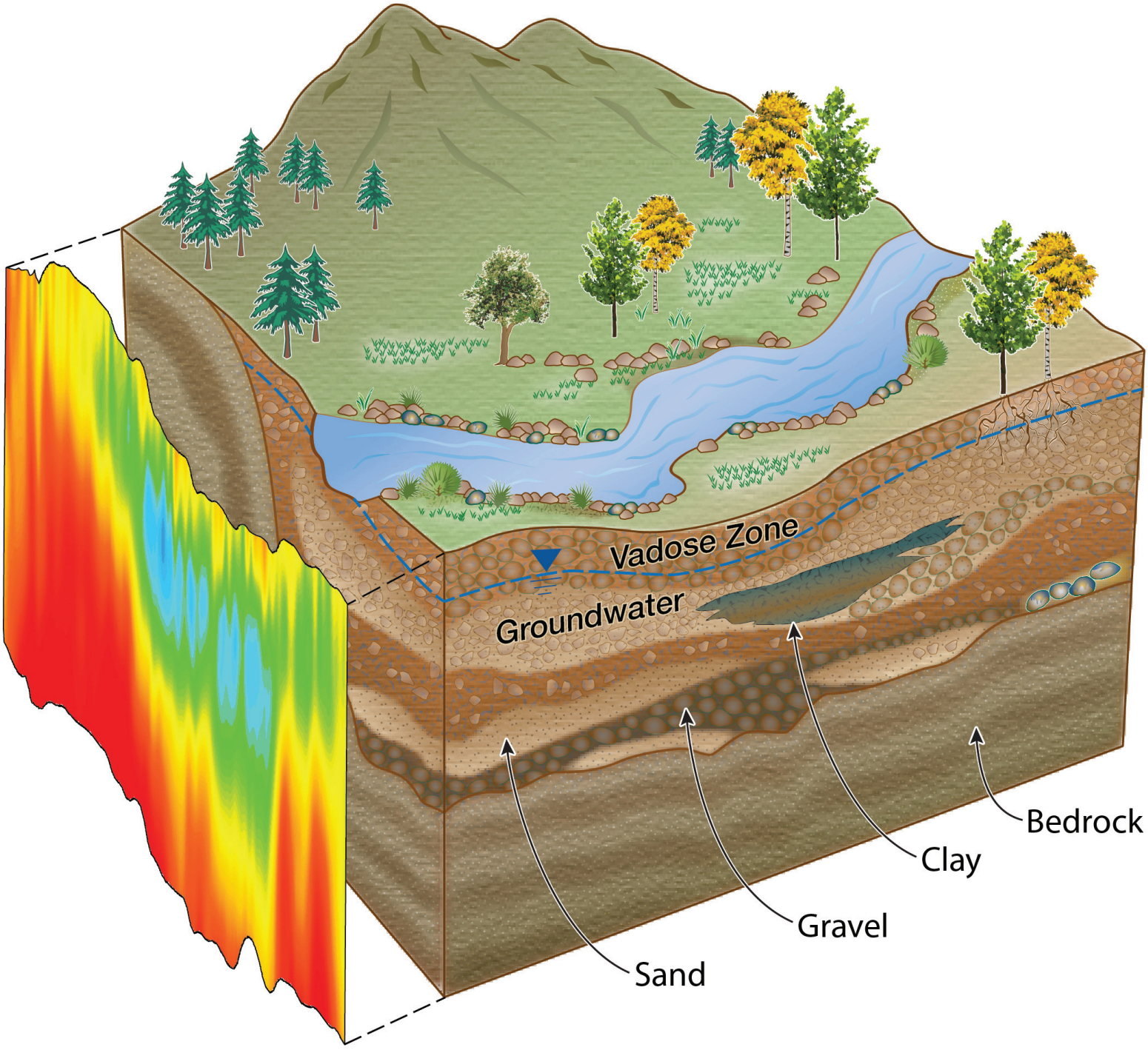
Vadose Zone
Groundwater
Sand
Gravel
Clay
Bedrock

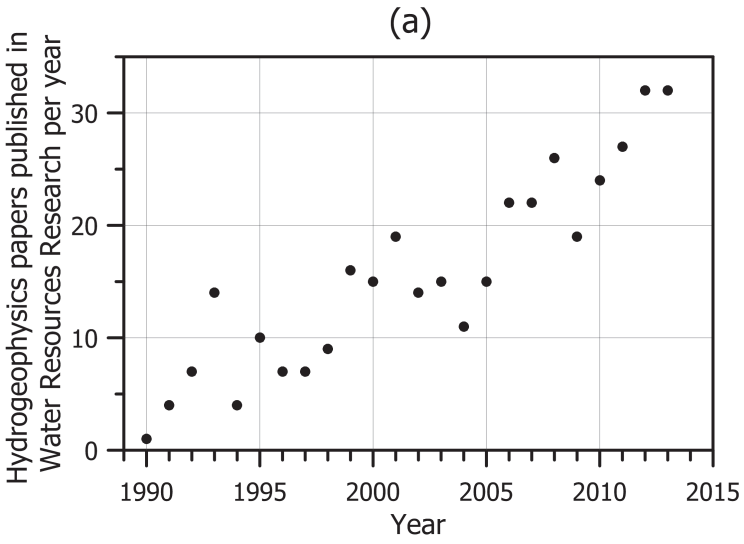
(a)
Hydrogeophysics papers published in Water Resources Research per year
0
10
20
30
1990
1995
2000
2005
2010
2015
Year

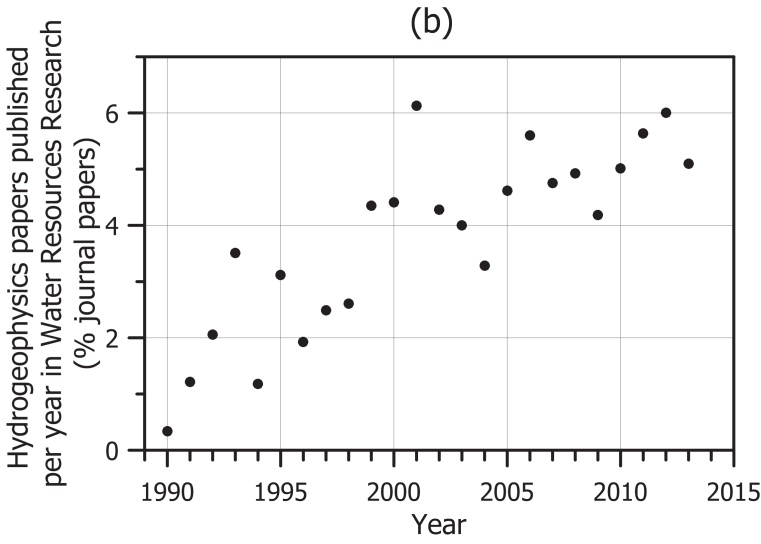
(b)
Hydrogeophysics papers published per year in Water Resources Research (% journal papers)
0
2
4
6
1990
1995
2000
2005
2010
2015
Year

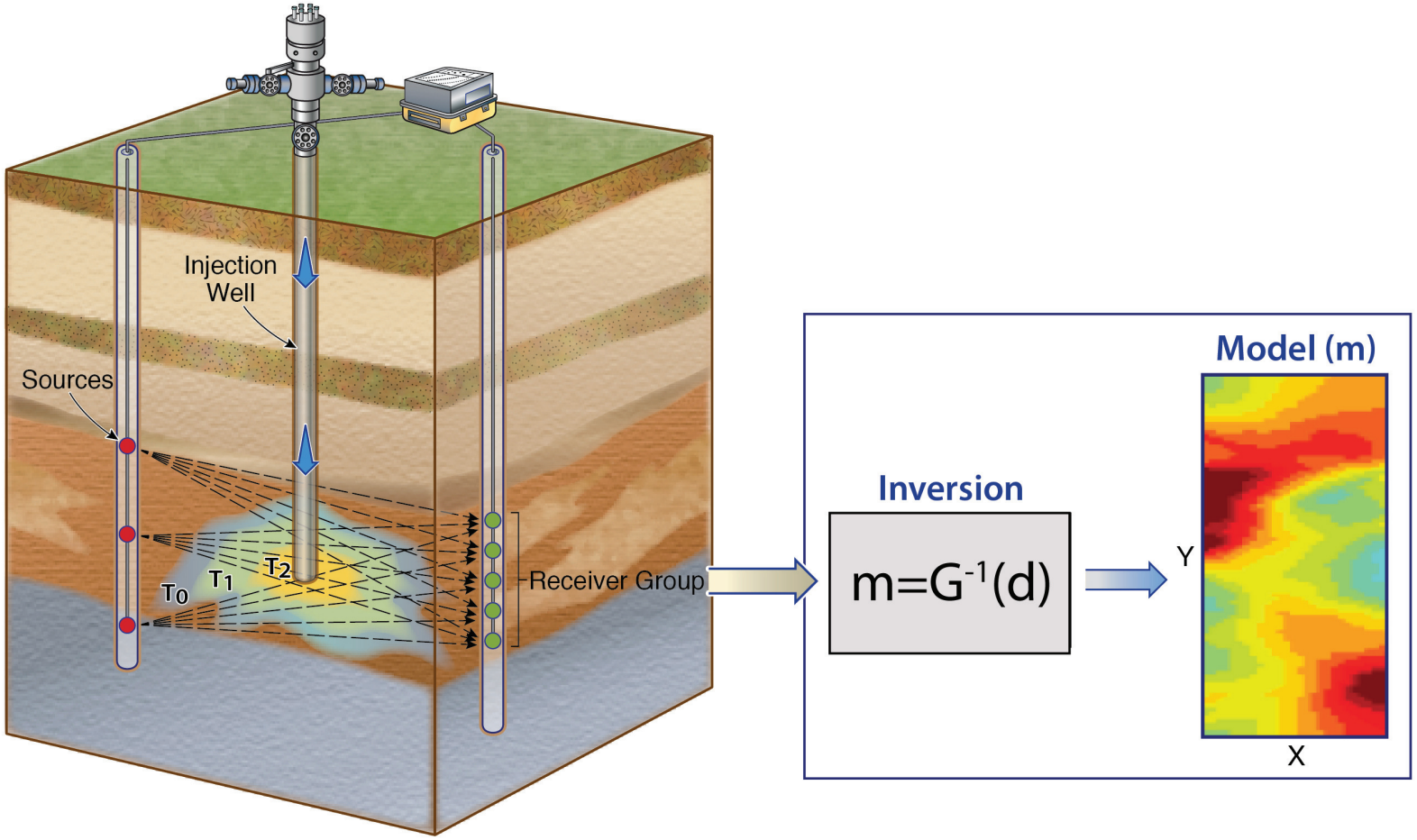
Injection Well
Sources
T0
T1
T2
Receiver Group
Inversion
m=G-1(d)
Model (m)
Y
X

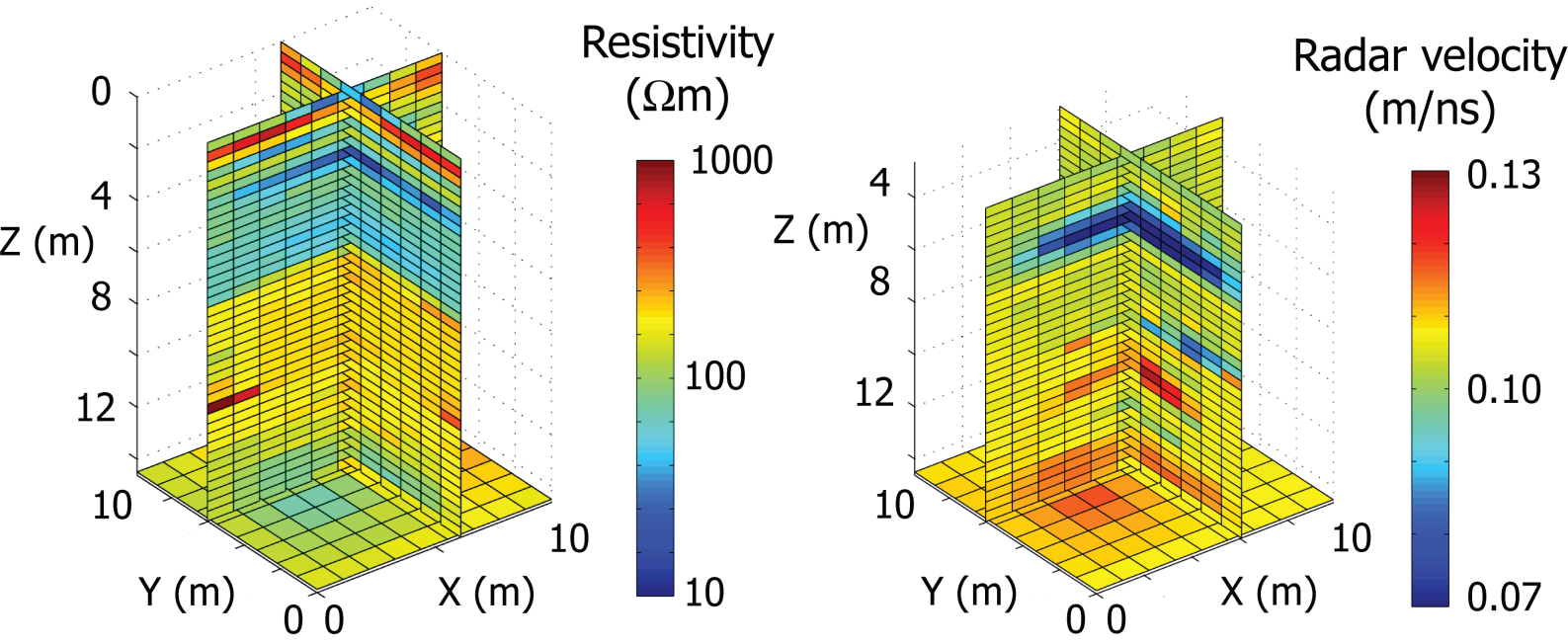
Resistivity
(Ωm)
1000
100
10
Z (m)
0
4
8
12
10
Y (m)
0 0
X (m)
10
Radar velocity
(m/ns)
0.13
0.10
0.07
Z (m)
4
8
12
10
Y (m)
0 0
X (m)
10

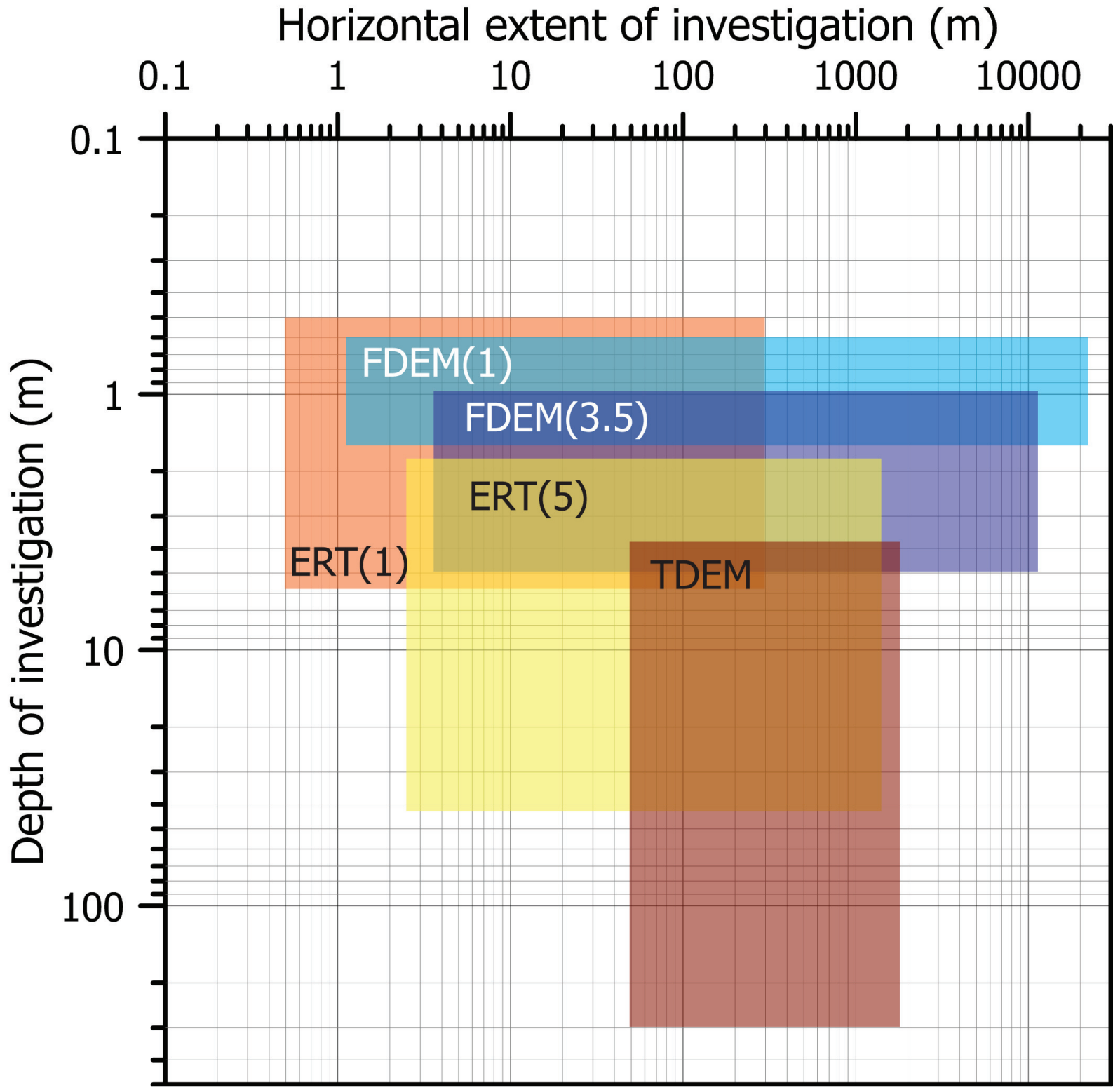
Horizontal extent of investigation (m)
0.1
1
10
100
1000
10000
Depth of investigation (m)
0.1
1
10
100
FDEM(1)
FDEM(3.5)
ERT(5)
ERT(1)
TDEM

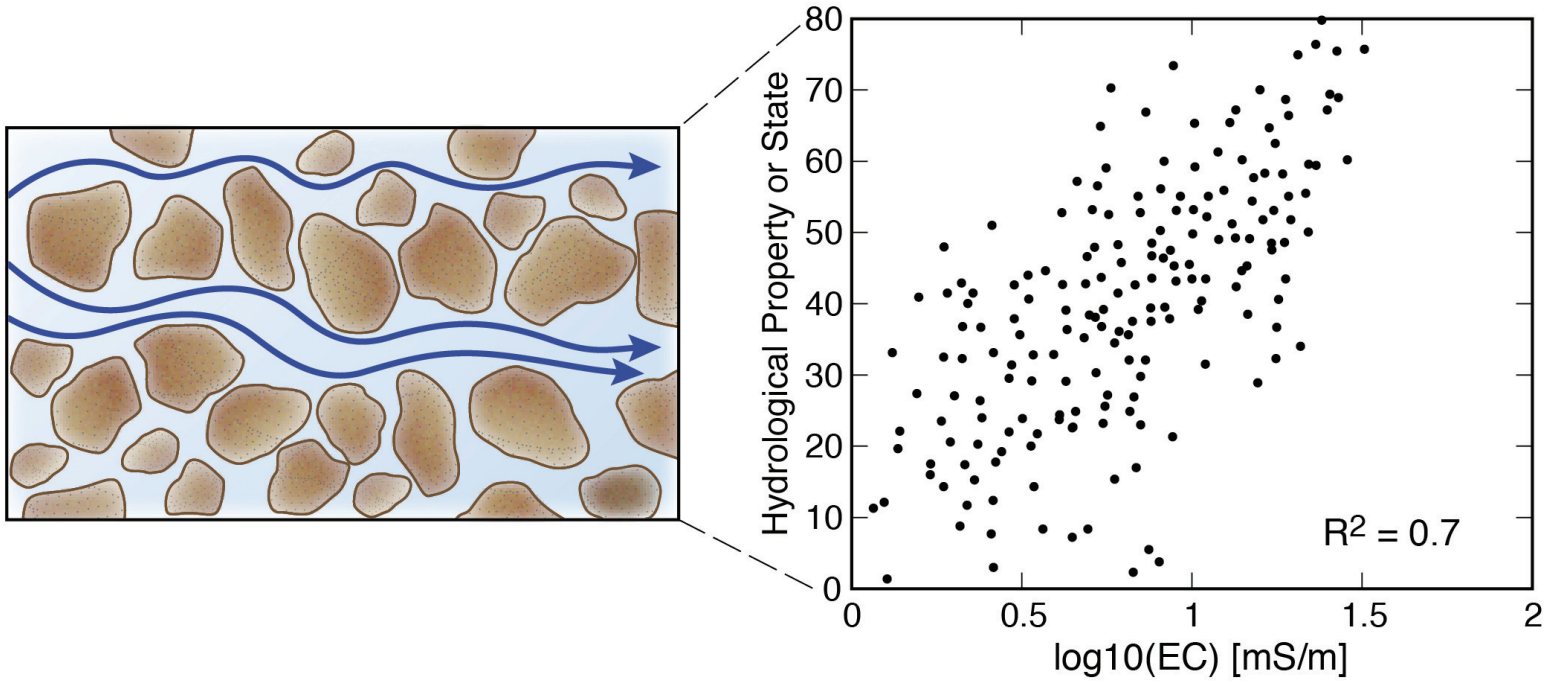
Hydrological Property or State
80
70
60
50
40
30
20
10
0
0
0.5
1
1.5
2
log10(EC) [mS/m]
R2 = 0.7

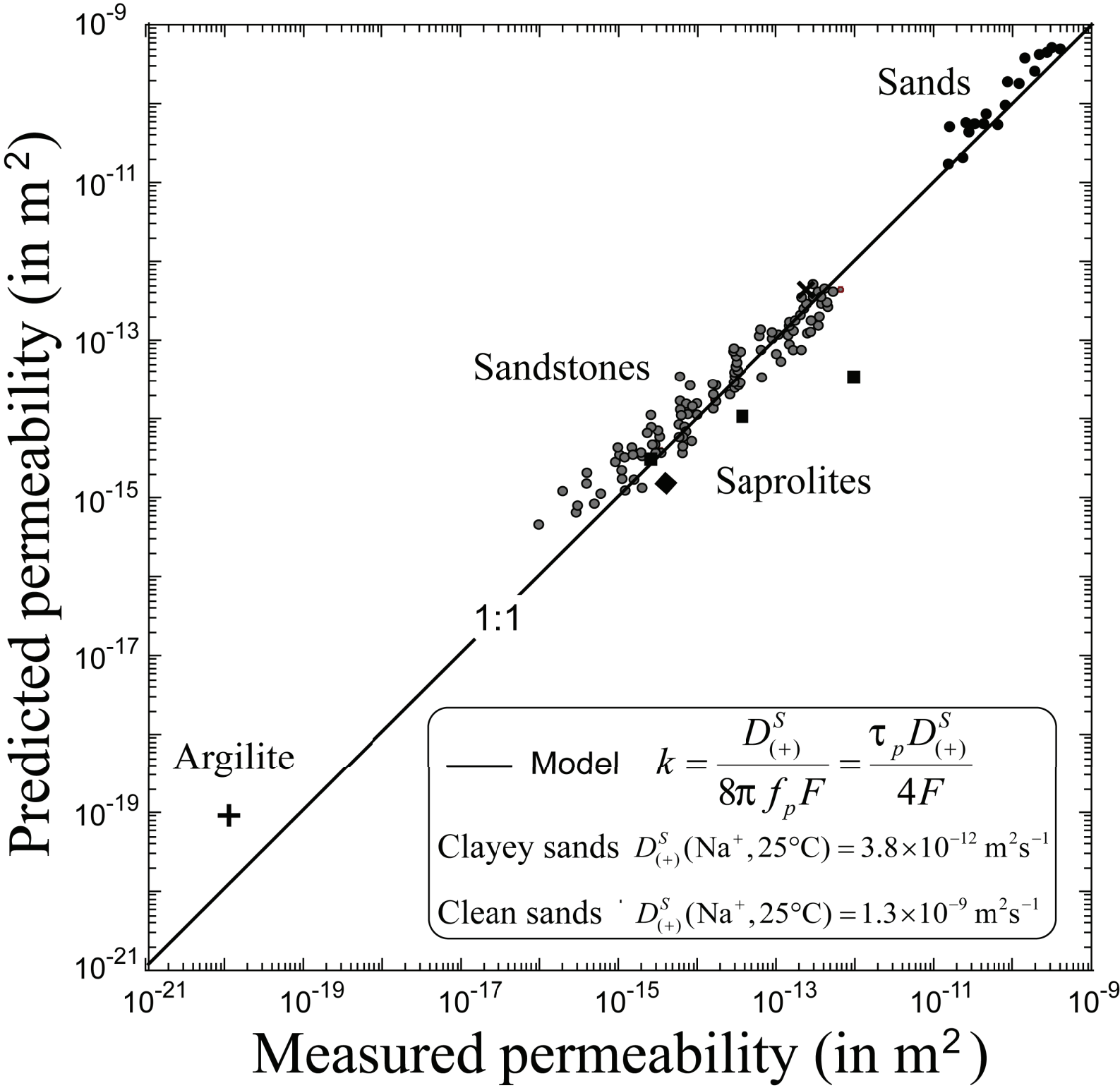
Predicted permeability (in m²)
Measured permeability (in m²)
10-9
10-11
10-13
10-15
10-17
10-19
10-21
Sands
Sandstones
Saprolites
Argilite
1:1
Model $k = \frac{D^S_{(+)}}{8\pi f_p F} = \frac{\tau_p D^S_{(+)}}{4F}$
Clayey sands $D^S_{(+)}(\mathrm{Na}^+, 25°\mathrm{C}) = 3.8\times10^{-12}\ \mathrm{m^2 s^{-1}}$
Clean sands $D^S_{(+)}(\mathrm{Na}^+, 25°\mathrm{C}) = 1.3\times10^{-9}\ \mathrm{m^2 s^{-1}}$

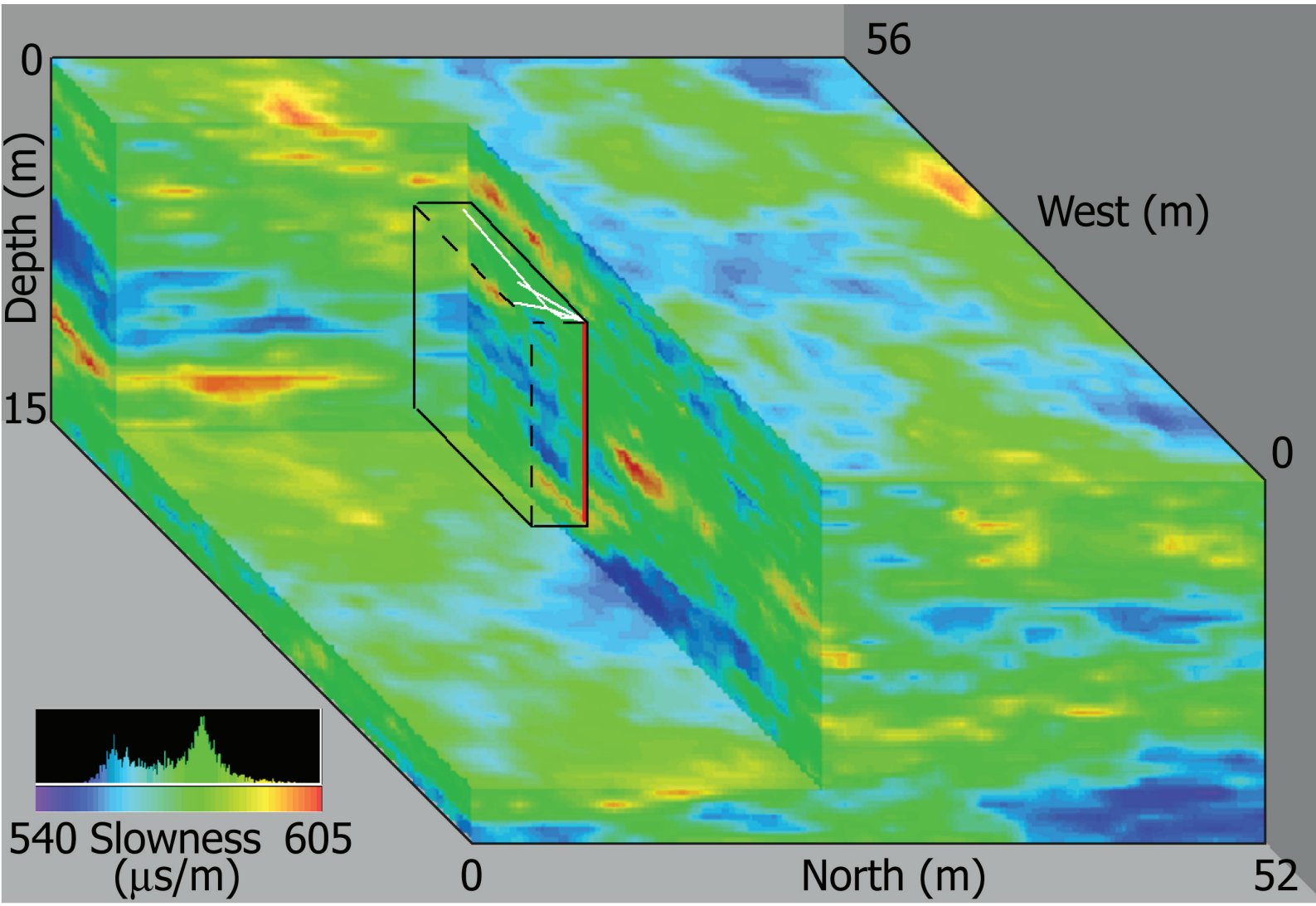
0
Depth (m)
15
56
West (m)
0
540 Slowness 605
(μs/m)
0
North (m)
52

Conditioned on borehole data

Conditioned on borehole and EMI data

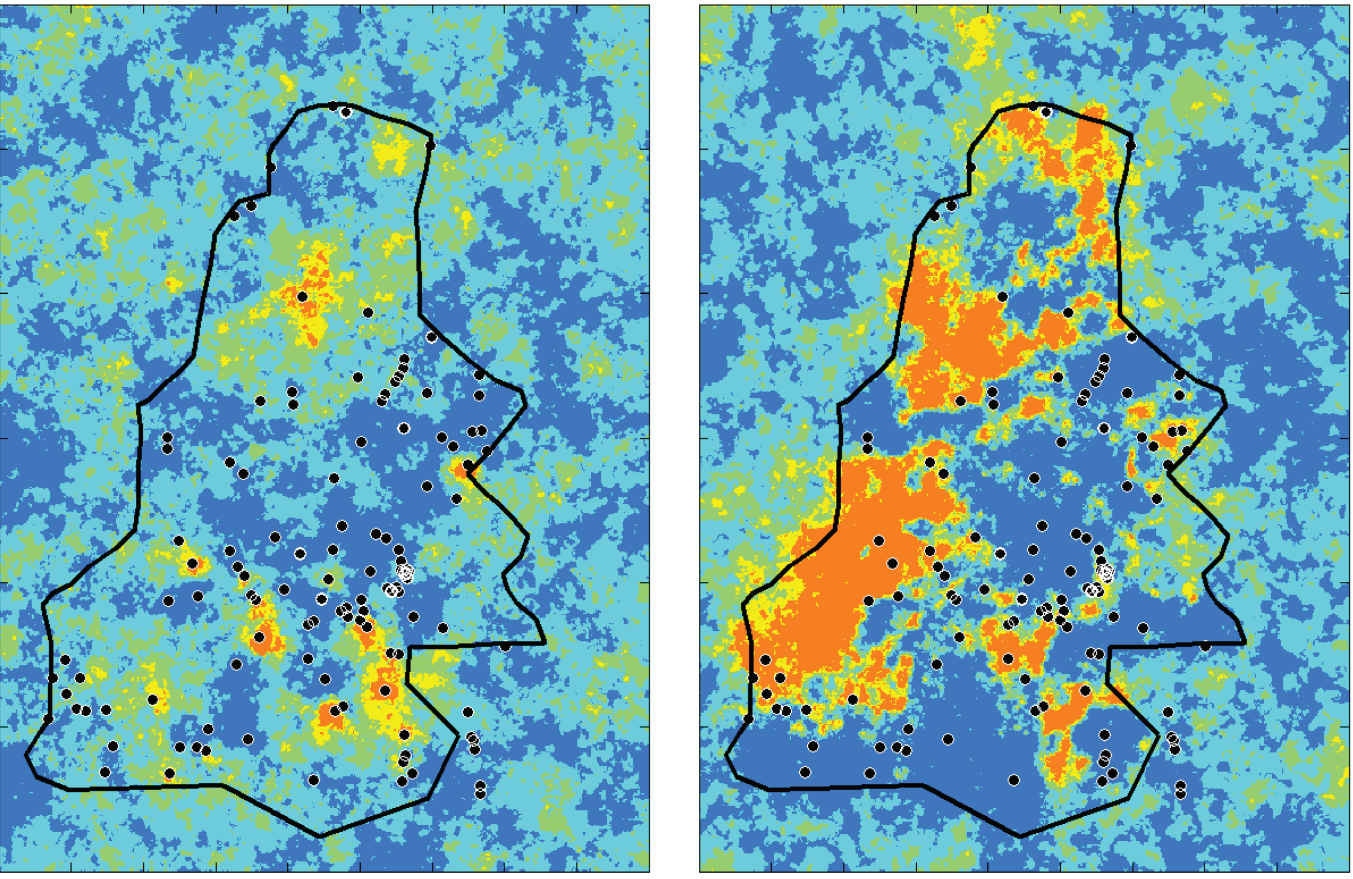

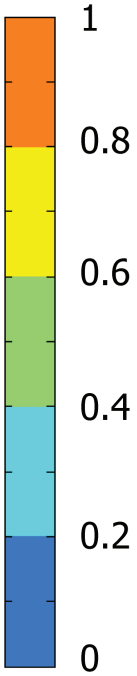

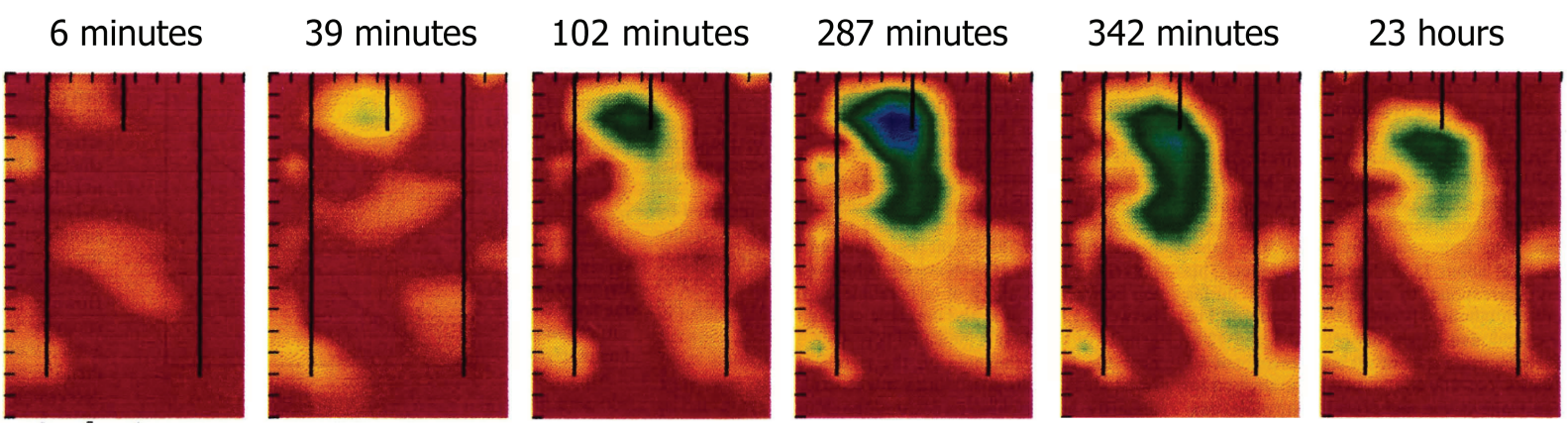
6 minutes
39 minutes
102 minutes
287 minutes
342 minutes
23 hours

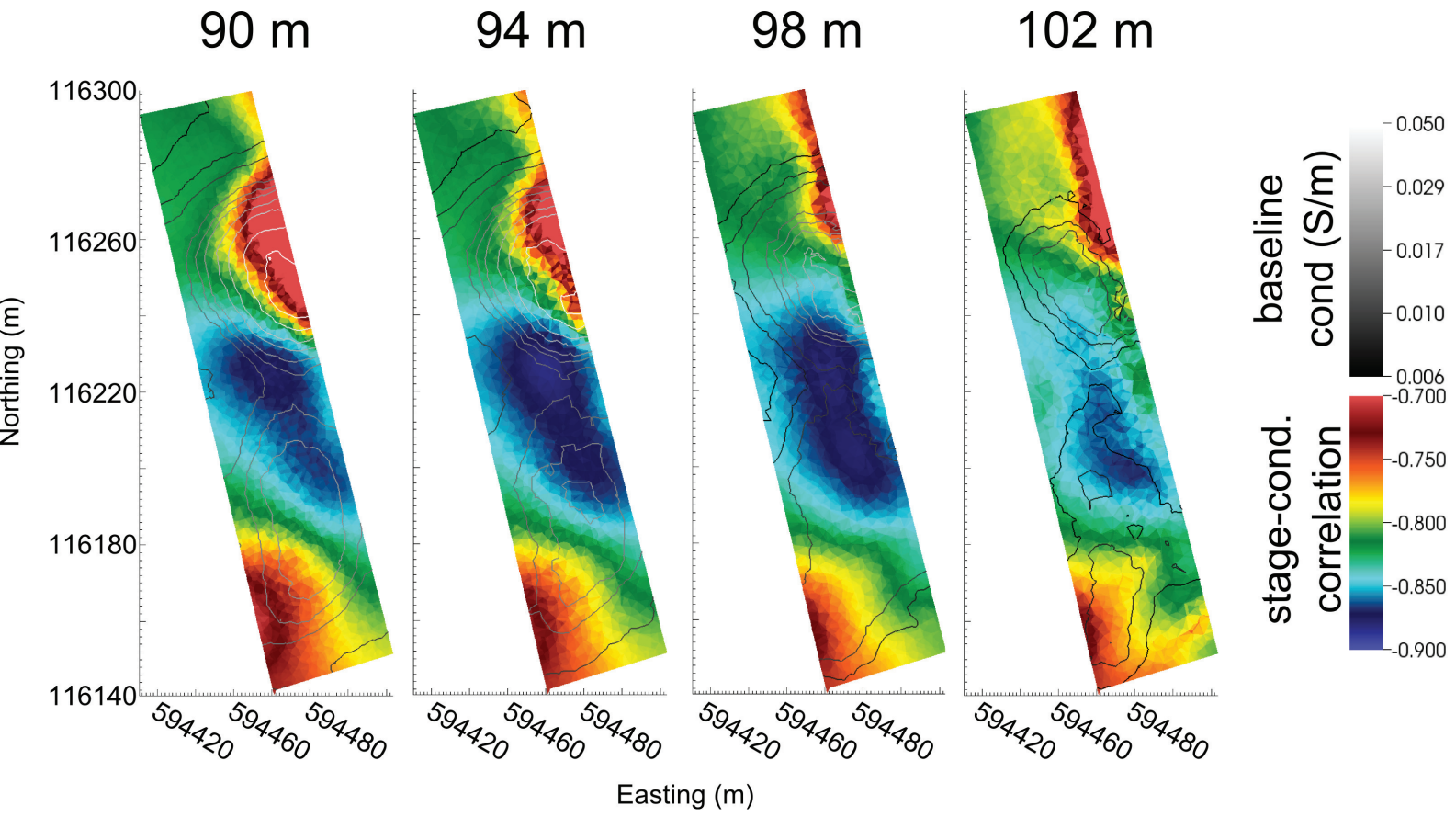
90 m
94 m
98 m
102 m
116300
116260
116220
116180
116140
Northing (m)
594420
594460
594480
Easting (m)
baseline cond (S/m)
0.050
0.029
0.017
0.010
0.006
stage-cond. correlation
-0.700
-0.750
-0.800
-0.850
-0.900

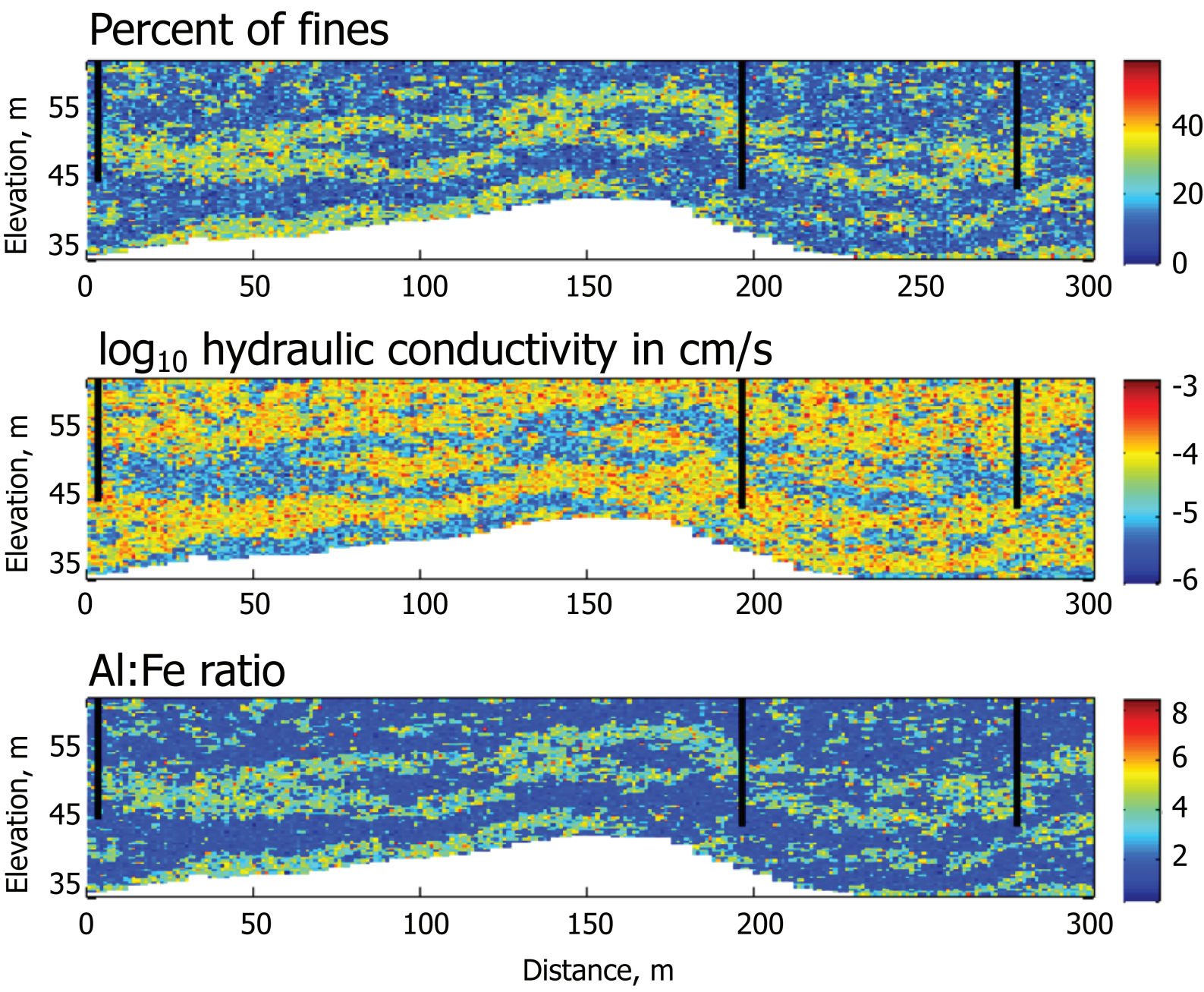
Percent of fines
Elevation, m
55
45
35
0
50
100
150
200
250
300
40
20
0
log10 hydraulic conductivity in cm/s
Elevation, m
55
45
35
0
50
100
150
200
300
-3
-4
-5
-6
Al:Fe ratio
Elevation, m
55
45
35
0
50
100
150
200
300
8
6
4
2
Distance, m

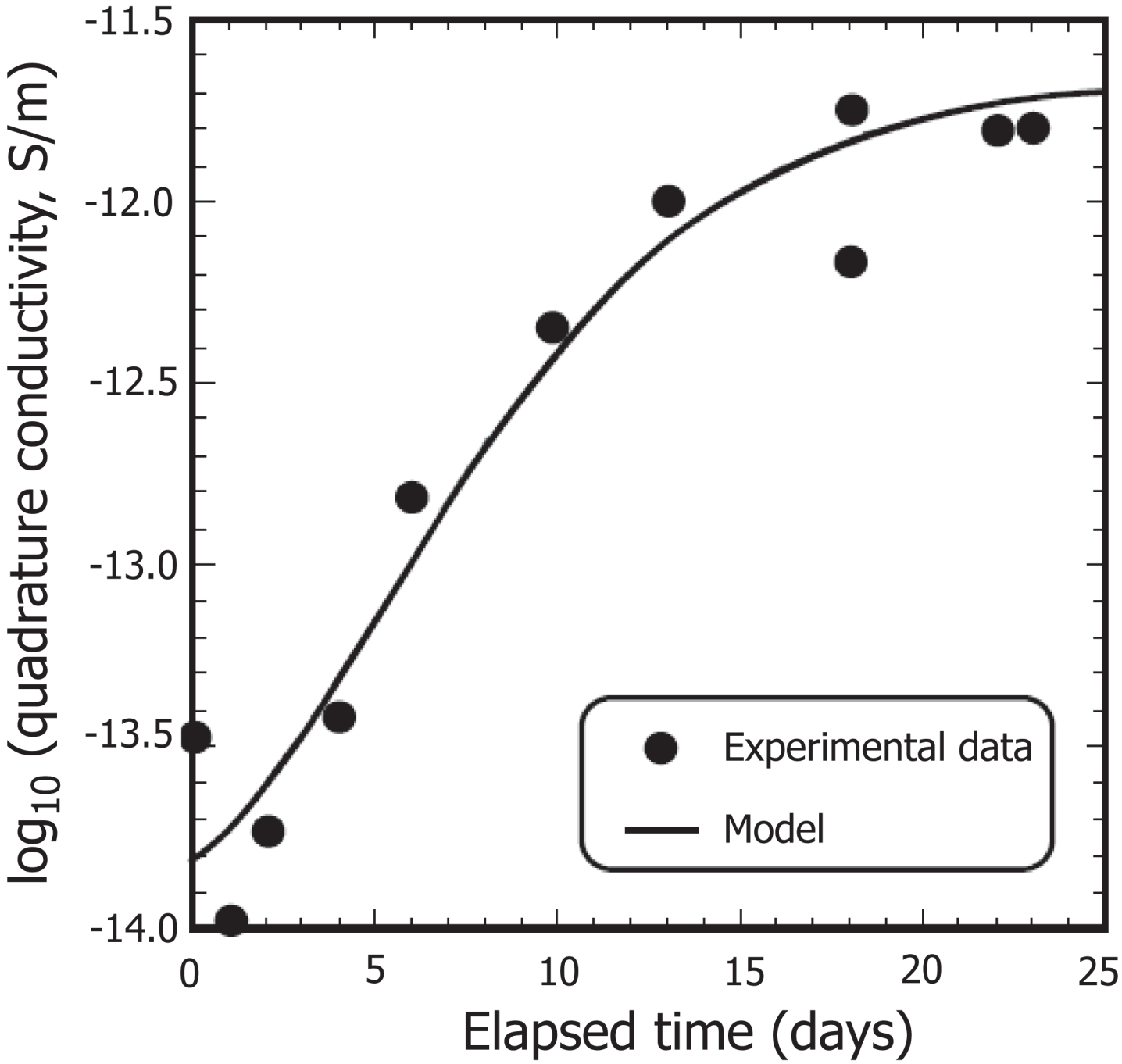
-11.5
-12.0
-12.5
-13.0
-13.5
-14.0
0
5
10
15
20
25
log10 (quadrature conductivity, S/m)
Elapsed time (days)
Experimental data
Model

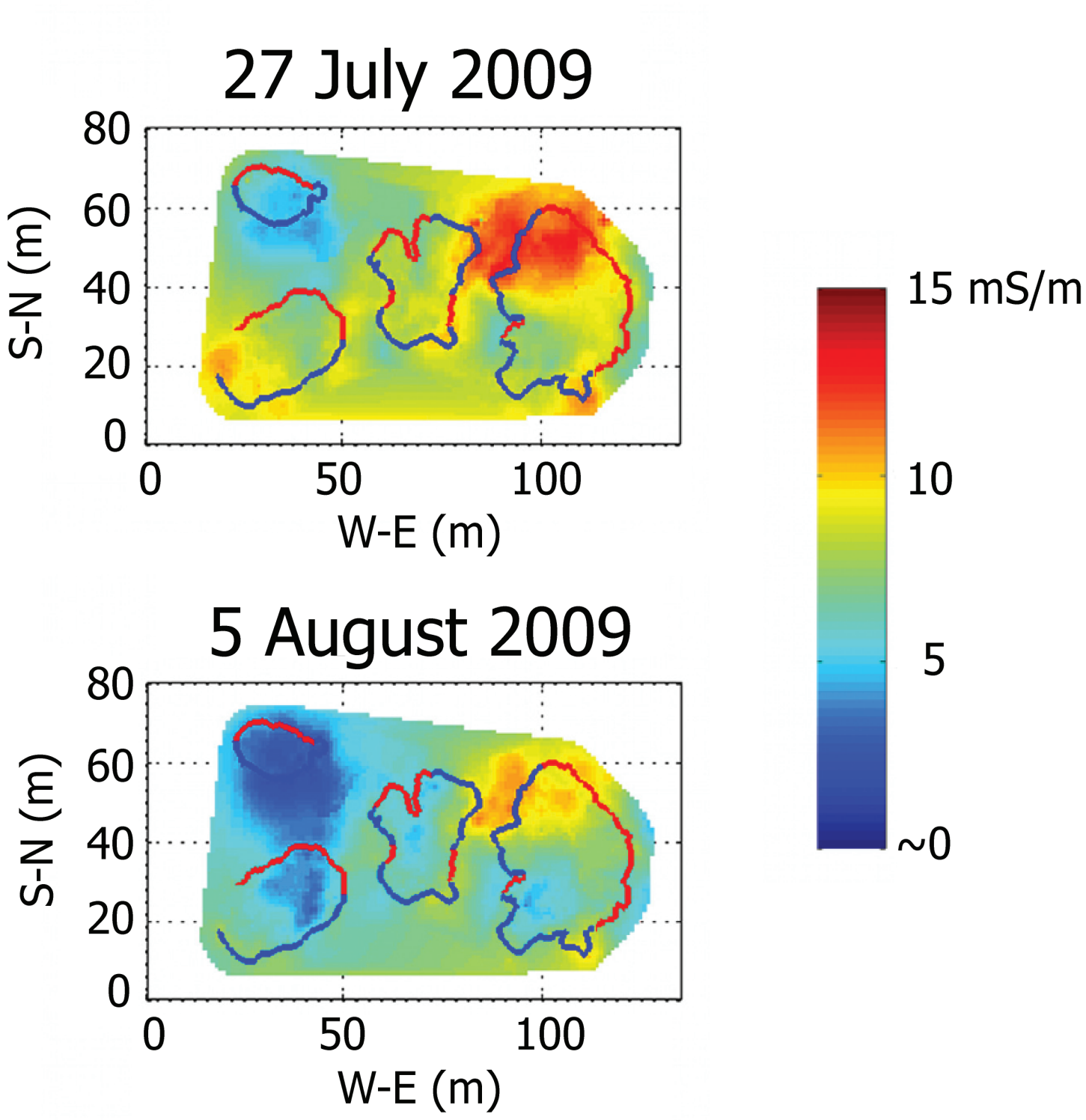
27 July 2009
S-N (m)
W-E (m)
0
20
40
60
80
0
50
100
5 August 2009
S-N (m)
W-E (m)
0
20
40
60
80
0
50
100
15 mS/m
10
5
~0

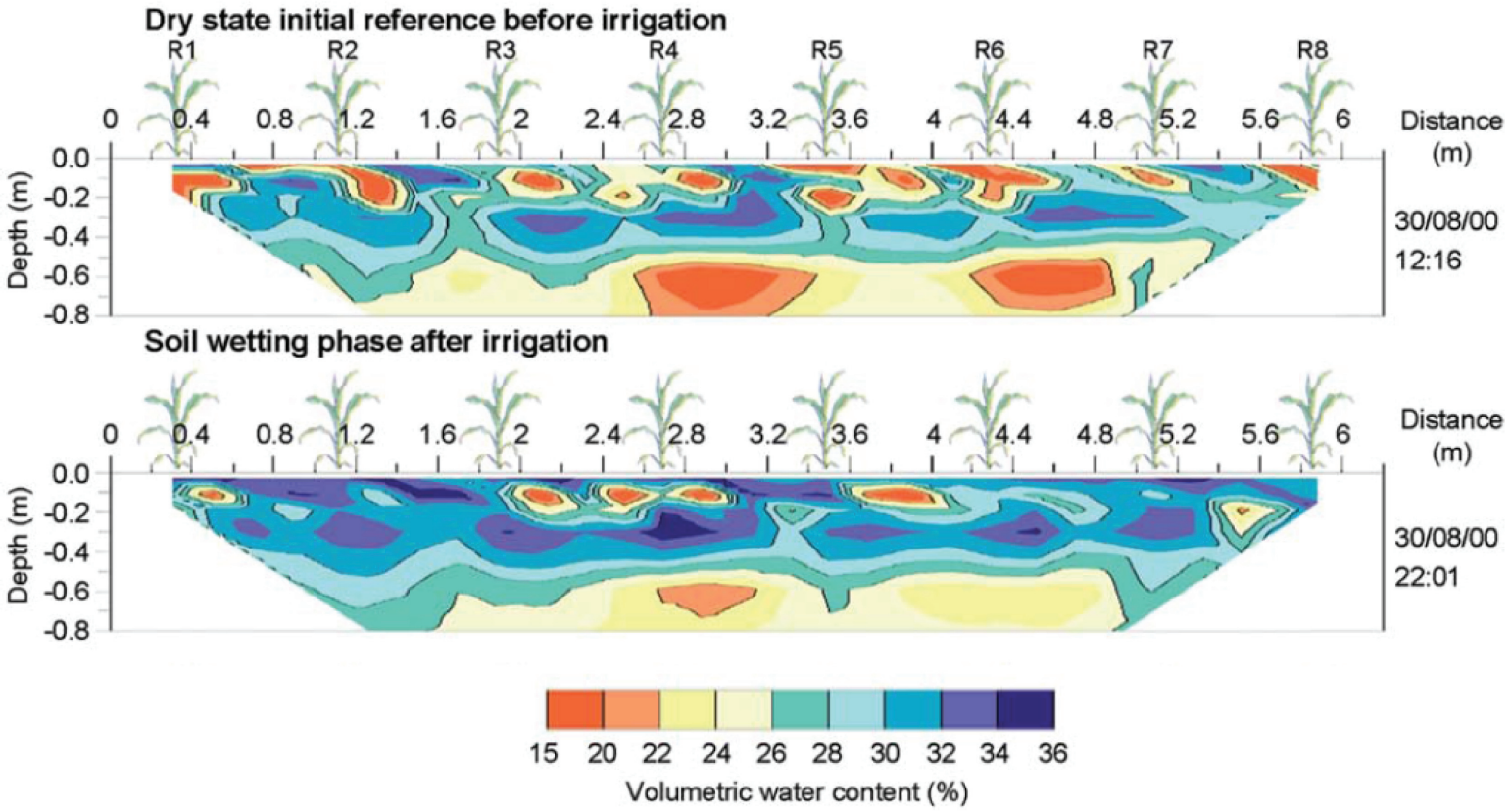
Dry state initial reference before irrigation
R1
R2
R3
R4
R5
R6
R7
R8
0
0.4
0.8
1.2
1.6
2
2.4
2.8
3.2
3.6
4
4.4
4.8
5.2
5.6
6
Distance (m)
Depth (m)
0.0
-0.2
-0.4
-0.6
-0.8
30/08/00
12:16
Soil wetting phase after irrigation
30/08/00
22:01
15
20
22
24
26
28
30
32
34
36
Volumetric water content (%)

TABLE 1: List of commonly used geophysical methods in hydrology and the geophysical properties they sense.

Geophysical method	**Geophysical properties**	**Examples of derived properties and states**
DC resistivity	Electrical conductivity	Water content, clay content, pore water conductivity
Induced polarization	Electrical conductivity, chargeability	Water content, clay content, pore water conductivity, surface area, permeability
Spectral induced polarization	As above but with frequency dependence	Water content, clay content, pore water conductivity, surface area, permeability, geochemical transformations
Self-potential	Electrical sources, electrical conductivity	Water flux, permeability
Electromagnetic induction	Electrical conductivity	Water content, clay content, salinity
Ground penetrating radar	Permittivity, electrical conductivity	Water content, porosity, stratigraphy
Seismic	Elastic moduli and bulk density	Lithology, ice content, cementation state, pore fluid substitution
Seismoelectrics	Electrical current density	Water content, permeability
Nuclear magnetic resonance	Proton density	Water content, permeability
Gravity	Bulk density	Water content, porosity